

2006

## Design and Implementation of 8 Bit Successive Approximation ADC at 1MHZ

Sesha Smuruti Akkinapally  
*University of Rhode Island*

Follow this and additional works at: <https://digitalcommons.uri.edu/theses>

Terms of Use

All rights reserved under copyright.

---

### Recommended Citation

Akkinapally, Sesha Smuruti, "Design and Implementation of 8 Bit Successive Approximation ADC at 1MHZ" (2006). *Open Access Master's Theses*. Paper 1001.  
<https://digitalcommons.uri.edu/theses/1001>

This Thesis is brought to you by the University of Rhode Island. It has been accepted for inclusion in Open Access Master's Theses by an authorized administrator of DigitalCommons@URI. For more information, please contact [digitalcommons-group@uri.edu](mailto:digitalcommons-group@uri.edu). For permission to reuse copyrighted content, contact the author directly.

DESIGN AND IMPLEMENTATION OF 8 BIT SUCCESSIVE  
APPROXIMATION ADC AT 1MHZ.

BY

SESHA SMRUTI AKKINAPALLY

A THESIS SUBMITTED IN PARTIAL FULFILLMENT OF THE  
REQUIREMENTS FOR THE DEGREE OF  
MASTER OF SCIENCE  
IN  
ELECTRICAL ENGINEERING

UNIVERSITY OF RHODE ISLAND

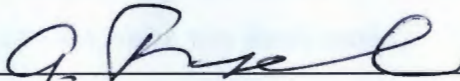
2006

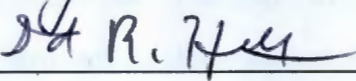
MASTER OF SCIENCE THESIS  
OF  
SESHA SMRUTI AKKINAPALLY

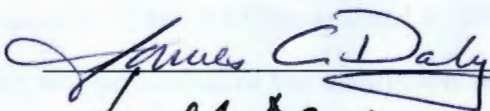
APPROVED:

Thesis Committee:

Major Professor

  
\_\_\_\_\_

  
\_\_\_\_\_

  
\_\_\_\_\_

  
\_\_\_\_\_  
DEAN OF THE GRADUATE SCHOOL

UNIVERSITY OF RHODE ISLAND

2006

## ABSTRACT

Successive Approximation Analog to Digital converters (ADCs) are very popular for reasonably quick conversion time and good resolution yet moderate circuit complexity. This thesis describes the design and implementation of a Successive Approximation ADC with 8-bit resolution at 1MHz speed in 0.5  $\mu\text{m}$  CMOS technology. Design, architecture, methodology and performance of the proposed ADC are presented.

The main features of the Successive Approximation (SAR) ADC architecture designed are very low power dissipation and small chip area because of the comparatively simple circuit implementation. The internal Digital to Analog Converter (DAC) is the most important block of the SAR ADC. Division of Charge implementation was used to realize the DAC to minimize the short-comings of the conventional charge-redistribution implementation. The SAR ADC was realized using Switched Capacitor circuitry. The hardware implementation of the schematic was done in MAGIC and the functionality of the ADC was tested in HSPICE. A test chip was fabricated and received for verification of the simulation results.

## ACKNOWLEDGMENTS

It is a pleasure to thank the many people who made this thesis possible.

I thank my major advisor, Dr. Godi Fischer, who helped me right from the conception of the idea to the very end of the thesis. I am grateful to Dr. Fischer for his guidance and support throughout the course of study. He is an instructor par excellence and I am privileged to work under his guidance.

Many thanks to my committee members: Dr. Fischer, Dr. Daly and Dr. Heskett; as well as my committee chair Dr. Natasha Thomas. I am very thankful to my professors: Dr. Kumaresan, Dr. Mitra, Dr. Sun and Dr. Davis. I'd also like to thank everyone I've had the pleasure to study and work with: Prasan, Vijay, Harini and Partha. I also thank the Department secretaries, Phyllis and Meredith for their help.

I am grateful to Michael Tedeschi, Edward Zanella, Naveen Lokam and Marie Crowley for giving me the opportunity to work at ON Semiconductor. I express my gratitude for their inputs from real world experience.

Finally, I am indebted to my parents, my sister and Bharath for the love and support they have given through the years. I thank them for giving me constant encouragement, inspiration and motivation without which my stay in United States and Master's study would not have been possible.

## TABLE OF CONTENTS

<b>ABSTRACT</b> . . . . .	ii
<b>ACKNOWLEDGMENTS</b> . . . . .	iii
<b>TABLE OF CONTENTS</b> . . . . .	iv
<b>LIST OF TABLES</b> . . . . .	vii
<b>LIST OF FIGURES</b> . . . . .	viii
<b>CHAPTER</b>	
<b>1 Introduction</b> . . . . .	1
1.1 Goal . . . . .	2
1.2 Thesis Organization . . . . .	3
List of References . . . . .	3
<b>2 Introduction to Analog to Digital Converters</b> . . . . .	4
2.1 Ideal Analog to Digital Converter (ADC) . . . . .	4
2.2 ADC Specifications . . . . .	6
2.2.1 Static Performance Measures . . . . .	6
2.2.2 Dynamic Performance Measures . . . . .	12
2.2.3 Frequency Domain Measures . . . . .	13
List of References . . . . .	15
<b>3 ADC Architectures</b> . . . . .	16
3.1 Different ADC Architectures . . . . .	16
3.1.1 Flash ADCs . . . . .	16

	<b>Page</b>
3.1.2 Subranging or Two-Step ADCs . . . . .	18
3.1.3 Pipelined ADCs . . . . .	19
3.1.4 Integrating ADCs . . . . .	21
3.1.5 Successive Approximation ADCs . . . . .	23
3.1.6 Sigma-Delta ADCs . . . . .	24
3.2 Comparison of Different Architectures . . . . .	26
3.3 Successive Approximation ADC . . . . .	27
3.3.1 DAC - Based Successive Approximation ADC . . . . .	29
List of References . . . . .	37
<b>4 Design and Implementation of SAR ADC . . . . .</b>	<b>38</b>
4.1 Implemented Architecture of SAR ADC . . . . .	38
4.2 Control Circuitry and Generation of Timing Signals . . . . .	40
4.3 Main Blocks of the Implemented SAR . . . . .	43
4.3.1 Accumulator . . . . .	44
4.3.2 Divide by 2 circuit . . . . .	46
4.3.3 Comparator . . . . .	53
4.3.4 Output Registers . . . . .	55
<b>5 Layout and Simulation Results . . . . .</b>	<b>56</b>
5.1 Layout Considerations . . . . .	56
5.1.1 Floor Planning . . . . .	56
5.1.2 Noise Considerations . . . . .	57
5.1.3 Matching Issues . . . . .	58
5.2 Simulation Results . . . . .	59

	<b>Page</b>
<b>6 Testing and Results</b> . . . . .	61
6.1 Required Equipment for Testing . . . . .	61
6.2 Testing Procedure and Results . . . . .	62
6.3 Conclusion . . . . .	66
List of References . . . . .	68
<b>BIBLIOGRAPHY</b> . . . . .	69



## LIST OF TABLES

<b>Table</b>		<b>Page</b>
1	Performance specifications . . . . .	51
2	Measured Digital output codes . . . . .	68
3		
4		
5		
6		
7		
8		
9		
10		
11		
12		
13		
14		
15		
16		
17		
18		
19		
20		

## LIST OF FIGURES

Figure		Page
1	Block diagram representing a Analog to Digital Converter (ADC) [1] . . . . .	4
2	(a) Transfer Curve for an ideal ADC and (b) its corresponding quantization error [2] . . . . .	5
3	Transfer Curve illustrating offset error . . . . .	7
4	Transfer Curve illustrating Gain error [2] . . . . .	8
5	Transfer Curve illustrating Accuracy [2] . . . . .	9
6	Transfer Curve illustrating INL error [2] . . . . .	10
7	Transfer Curve illustrating DNL error [2] . . . . .	11
8	Transfer Curve illustrating Missing Codes . . . . .	12
9	SFDR Illustration . . . . .	14
10	Flash ADC . . . . .	17
11	subranging converters . . . . .	18
12	Pipelined Converters . . . . .	20
13	Integrating Converter ADC . . . . .	21
14	Behavior of Integrating Converter ADC . . . . .	22
15	Successive Approximation . . . . .	23
16	Sigma-Delta Converter . . . . .	24
17	Comparison of Different ADC architectures. . . . .	26
18	Flow graph illustrating binary search algorithm [2] . . . . .	28
19	3-bit R-2R ladder DAC . . . . .	29
20	3-bit charge redistribution DAC . . . . .	31

Figure		Page
21	The working of charge division by 2 circuit . . . . .	35
22	The implemented architecture of the SAR ADC . . . . .	38
23	The conversion process of the SAR ADC . . . . .	39
24	The non-overlapping nature of the clocks . . . . .	41
25	The control circuitry for the generation of non-overlapping clock signals . . . . .	41
26	The combinational logic implemented to generate the timing signals . . . . .	42
27	The timing signals . . . . .	43
28	The circuit implementation of the Accumulator . . . . .	44
29	The divide by 2 circuit implementation . . . . .	47
30	Simulation results of the accumulator and the divide by 2 circuit . . . . .	48
31	The circuit implementation of the transconductance op-amp . . . . .	49
32	Simulation results with the performance metrics of the op-amp . . . . .	52
33	The circuit implementation of Latched Comparator. . . . .	53
34	The simulation results of the comparator . . . . .	54
35	The Floor Planning implemented . . . . .	56
36	Figure illustrating common centroid layout . . . . .	58
37	The simulation results of SAR ADC . . . . .	59
38	Figure illustrating the complete layout with bonding pads . . . . .	60
39	DC test set up . . . . .	62
40	Graph illustrating the Error in LSB's . . . . .	63
41	AC Test set-up . . . . .	63
42	Figures Illustrating the SNR of the test chip . . . . .	65

**Figure**

**Page**

43 Histogram plot . . . . . 66

44 FFT of Spice Extracted File . . . . . 67

## CHAPTER 1

### Introduction

The growth in Digital Computing and Digital Signal Processing in the electronics world is usually referred as "*the world is becoming digital day by day.*" Digital circuits are less sensitive to the noise and exhibit more robustness to the increasing variations of the process and supply voltages, they also allow comparatively easier test automation when compared to the analog circuits. Hence the information is being increasingly stored, processed and communicated in the digital domain [1]. In our physical environment, naturally occurring signals are analog, hence a device that converts these analog signals to digital form is essential. An Analog to Digital Converter (ADC) converts a continuous signal into binary information. Thus, Analog to Digital Converters and their counterparts the Digital to Analog Converters are critical building blocks or sometimes even bottle necks in many applications.

An overwhelming variety of ADCs exist in the market today, with different resolutions, bandwidths, accuracies, architectures, packaging, power requirements, and temperature ranges, as well as variety of specifications, covering a broad range of performance needs. There also exists a variety of applications in Data Acquisition, Precision Measurement Applications, Communications, Instrumentation and Interfacing for Signal Processing etc. Depending upon the application, there is always a "best choice" of a particular type of ADC because of a clear cut advantage rather than any available ADC model. Thus, there is always an increasing need for further improvement of available ADC models.

## 1.1 Goal

The objective of this thesis is to design and implement an 8-bit Successive Approximation Analog to Digital Converter at 1 MHz speed compatible with 0.5 $\mu$ m CMOS process. The main features of this ADC are

- Simple Circuit implementation
- Small Die Size due to reduced number of capacitors in the internal DAC
- Low power dissipation
- Low to medium supply voltage (2-5V)

Successive Approximation (SAR) ADC's are preferred to other ADC architectures due to decreased power dissipation and small chip area because of the comparatively simple circuit implementation. The most important block of an SAR ADC is the internal Digital to Analog Converter (DAC). The linearity of the SAR ADC depends on the linearity of the DAC unlike the other ADC architectures [2].

Most of the previous implementations of the SAR ADCs used the conventional R-2R architecture to implement the internal DAC [2]. The R-2R architecture inherently suffers from DNL (Differential Non-Linearity) and INL (Integral Non-Linearity) errors, due to the mismatch in the resistors comprising the R-2R ladder.

The ADC's are usually classified based on three main features: the Chip Area, Speed and the Power dissipation. Chip area and the Power dissipation of an R-2R architecture increase as the resolution increases, due to the large resistor ladder realized, which also affects the speed of the ADC. In the Literature studied, few of these draw-backs have been overcome by the Charge-Redistribution implementation [2]. This architecture uses a Programmable Capacitor Array (PCA) to realize the DAC. As in R-2R architecture, the Capacitor Array grows as the resolution increases, thus the power dissipation and the circuit area also increases. Large input

capacitance has an effect on the Speed of the ADC, thus this architecture limits the resolution of the DAC to a maximum of 6-8 bits. The proposed Divide-by-2 Circuit overcomes these limitations. In the proposed architecture, irrespective of the resolution of the ADC, the number of capacitors required to implement the Divide-by-2 circuit do not increase. Thus, due to the reduced input capacitance, the Chip Area and the Power Dissipation are greatly reduced when compared to the conventional SAR ADC architectures. Speed of the proposed architecture is also reasonably good when compared to conventional architectures.

## 1.2 Thesis Organization

The thesis work is divided into 6 Chapters. Starting with the introduction, in the chapter 1; Chapter 2 illustrates the basic Analog to Digital Converter ADC and its performance measures. Chapter 3 will talk about the different ADC architectures available and the different methodologies existing to design a Successive Approximation ADC. Chapter 4 presents the conversion principle implemented and will describe the different blocks of the proposed ADC architecture in detail with the simulation results. Chapter 5 will discuss the layout considerations and the simulation results of the of the proposed ADC architecture. Chapter 6 describes the Testing procedure of the Test Chip and also presents the measured test results. Finally, it draws some conclusions.

## List of References

- [1] B. Razavi, *Data Conversion System Design*. New York, United States of America: IEEE Press, 1995.
- [2] K. M. David A. Johns, *Analog Integrated Circuit Design*. New York, United States of America: John Wiley and Sons, 1997.

## CHAPTER 2

### Introduction to Analog to Digital Converters

The basic definition of an ideal Analog to Digital Converter (ADC) and its transfer curve are presented in the first part of chapter. The second part of the chapter classifies and defines different ADC performance parameters. These parameters evaluate ADC's performance and thus help the designer to choose an appropriate architecture for a specific application.

#### 2.1 Ideal Analog to Digital Converter (ADC)

The block diagram representing a basic Analog to Digital Converter is shown in Figure 1. In the figure, Bout is the digital output word, Vin and Vref are the analog input and the reference signals respectively. The analog input and the digital output word are related by the following equation.

$$V_{ref}(b_1 2^{-1} + b_2 2^{-2} + \dots + b_N 2^{-N}) = V_{in} + (-)V_X \quad \dots (1)$$

$$\text{Where} \quad \left(\frac{1}{2}\right)V_{LSB} \leq V_X < \left(\frac{1}{2}\right)V_{LSB}$$

$V_{LSB}$  is defined as the change corresponding to a single Least Significant Bit(LSB) change.

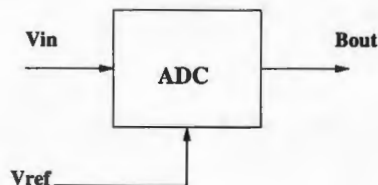


Figure 1. Block diagram representing a Analog to Digital Converter (ADC) [1]



The input-output transfer curve of an ideal 3-bit ADC is shown in Figure 2(a). Since the input signal is a continuous signal and the output is discrete, the transfer curve of the ADC resembles that of a staircase. The Figure illustrates that there are  $2^N$  quantization levels, where  $N$  is the number of bits in the digital output.

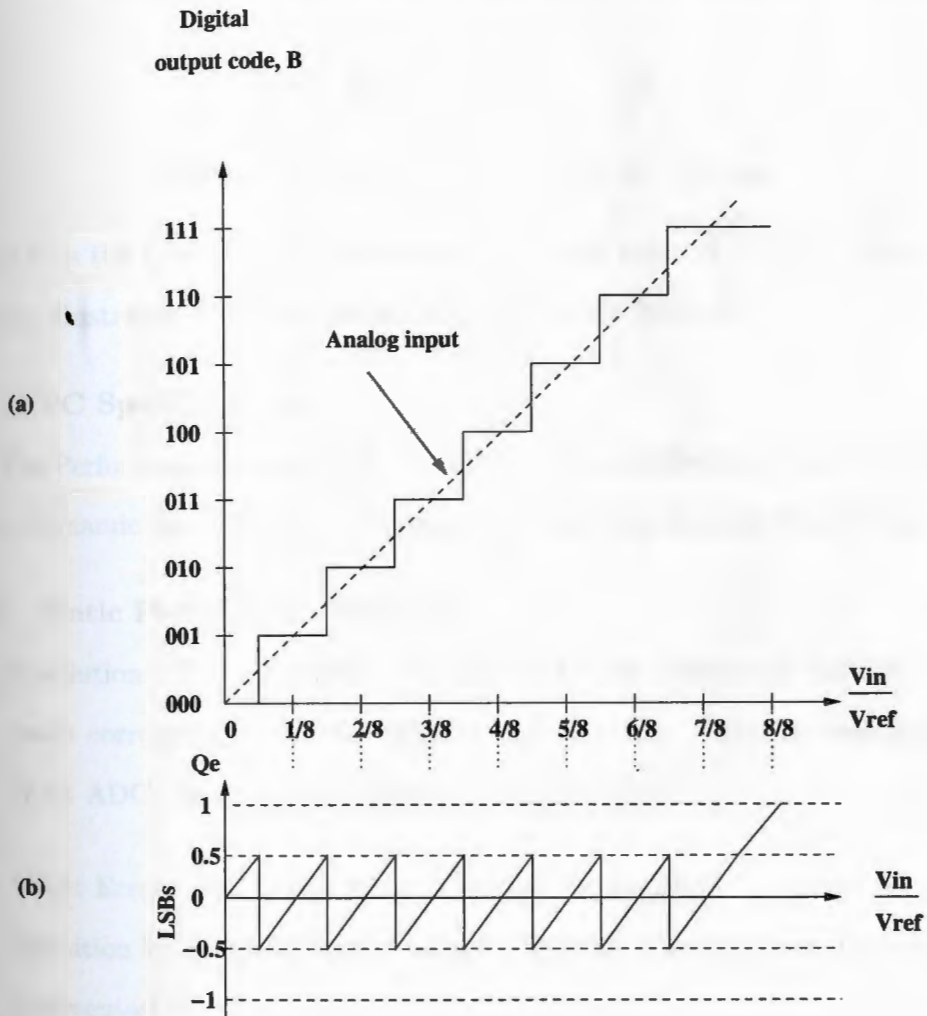


Figure 2. (a) Transfer Curve for an ideal ADC and (b) its corresponding quantization error [2]

- **Quantization Error:** As a range of valid input values produce the same digital output word, signal ambiguity results and is referred to as the Quantization error  $Q_e$ . This error is defined as the difference between the actual analog input and the value of the output given in voltage [3].

$$Q_e = V_{in} - V_{staircase} \dots\dots (2)$$

$$\text{Where } V_{staircase} = D \cdot \left(\frac{V_{ref}}{2^N}\right) = D \cdot V_{LSB}$$

Where D is the Digital output code and  $V_{LSB}$  is the value of 1 LSB in volts. Figure 2(b) illustrates the Quantization error of an ideal 3-bit ADC.

## 2.2 ADC Specifications

The Performance measures of an ADC can be classified into three categories: Static, Dynamic and Frequency Domain. The following sections detail them.

### 2.2.1 Static Performance Measures

- **Resolution:** The resolution is defined to be the number of distinct analog levels corresponding to the different digital words. Thus, by definition, an N-bit ADC can resolve  $2^N$  distinct analog levels [1].
- **Offset Error:** The Offset Error is defined as the deviation of the first code transition  $V_{0...01}$  from the ideal value of LSB [1]. This can be mathematically represented as

$$E_{offset} = \left(\frac{V_{0...01}}{V_{staircase}}\right) - LSB \dots\dots (3)$$

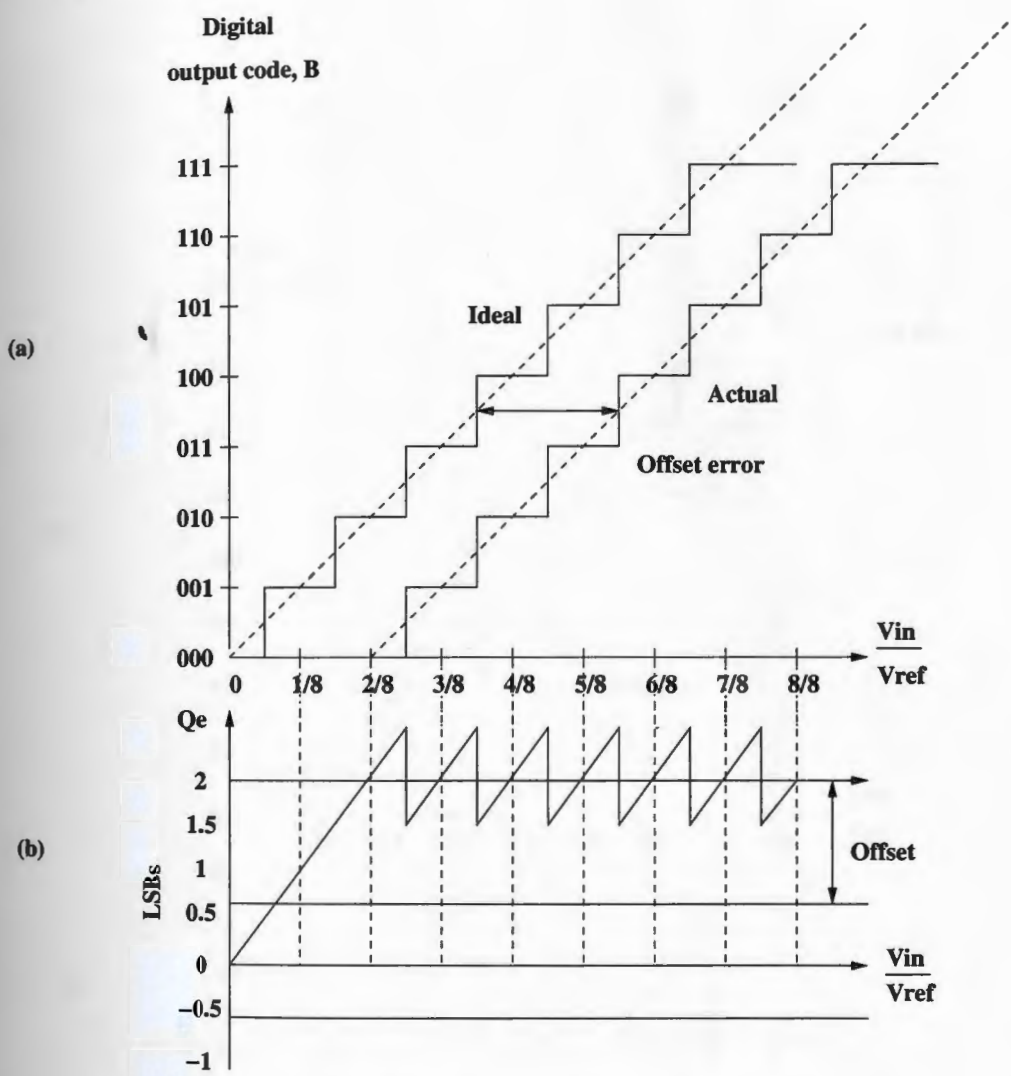


Figure 3. Transfer Curve illustrating offset error

- Gain Error: The Gain error is defined to be the difference at the full-scale value between the ideal and actual curves when the offset error has been reduced to zero [1]. The Gain error for an ADC can be mathematically represented as

$$E_{gain} = \left[ \left( \frac{V_{1\dots1}}{V_{LSB}} \right) - \left( \frac{V_{0\dots01}}{V_{LSB}} \right) \right] - (2^N - 2) \dots (4)$$

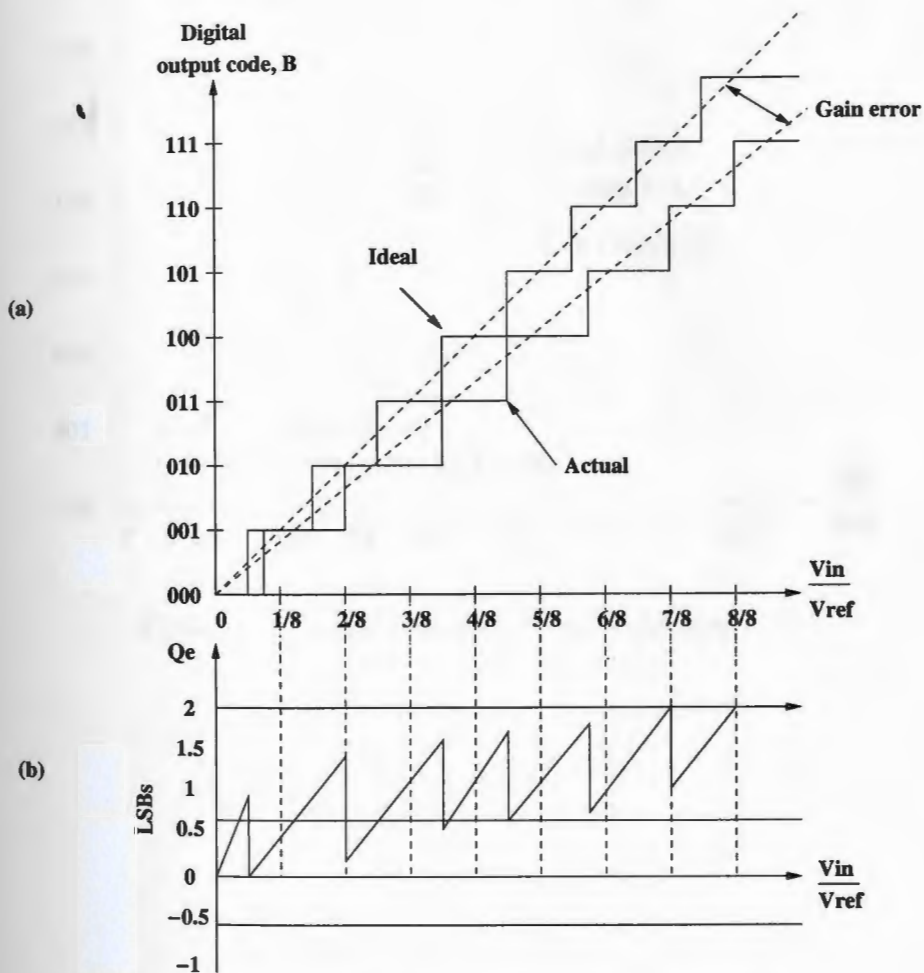


Figure 4. Transfer Curve illustrating Gain error [2]

- Accuracy: The absolute accuracy of a converter is defined to be the difference between the expected and actual transfer responses [1]. The absolute accuracy includes the offset, gain and the linearity errors.

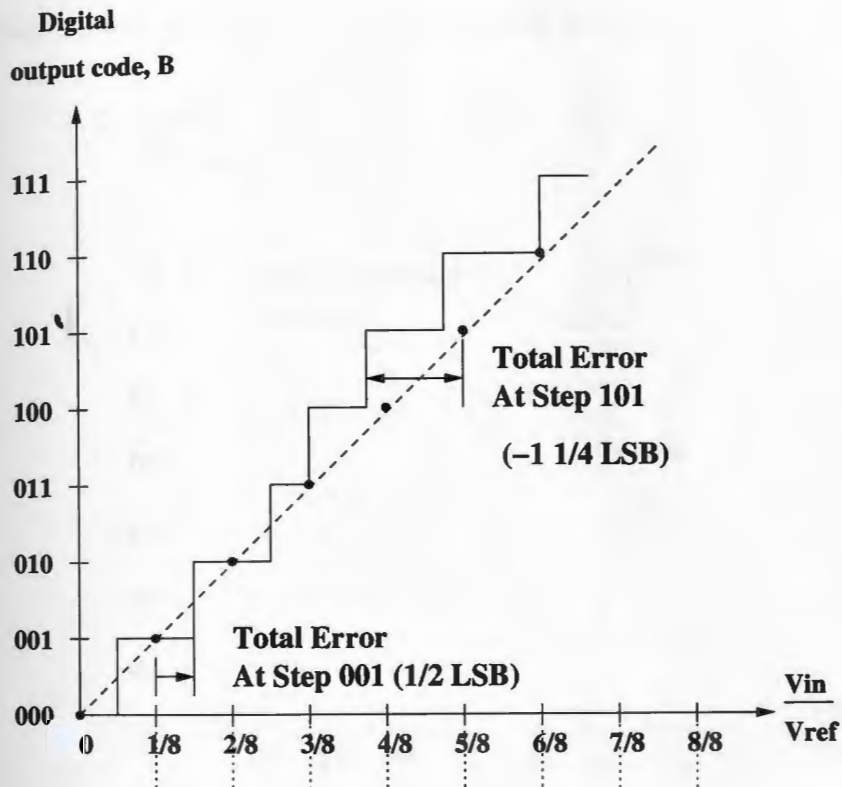


Figure 5. Transfer Curve illustrating Accuracy [2]

- **Integral Nonlinearity Error(INL):** The Integral Nonlinearity Error is defined as the deviation from a straight line (ideal) after the offset and gain error have been corrected [1]. Conventionally, a "best-fit" straight line is drawn through the end points of the first and the last code transition to define the straight (ideal) line. The Figure 5 illustrates the INL.

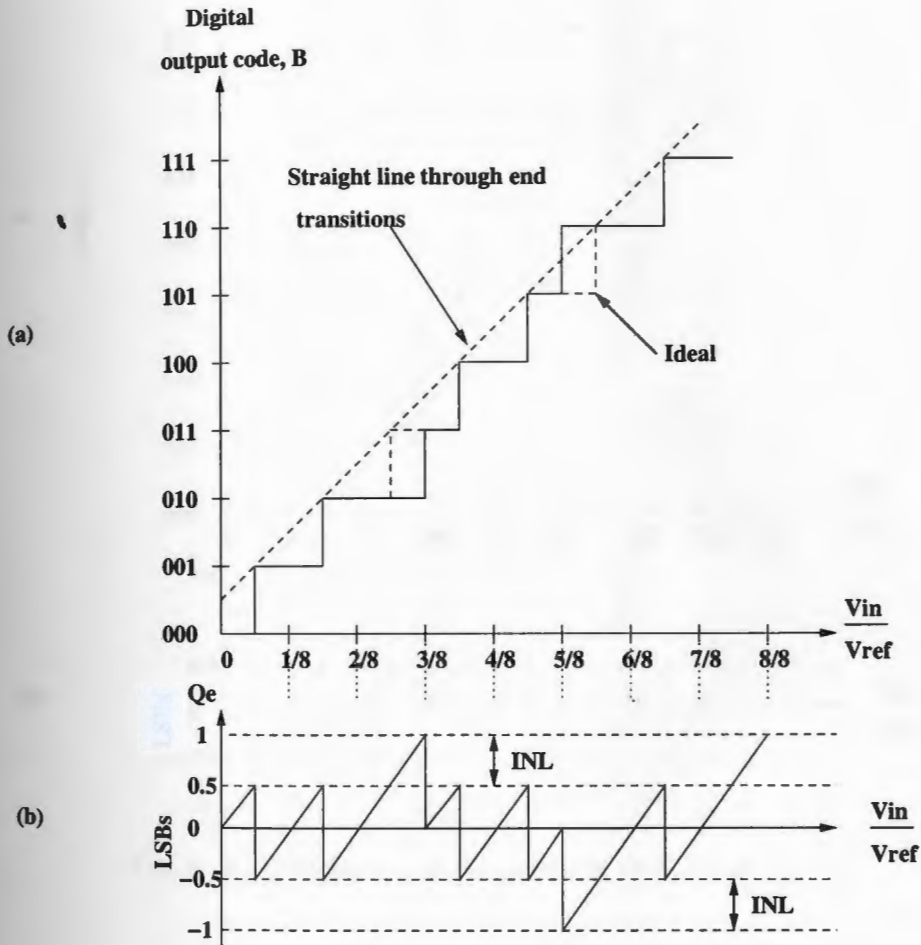


Figure 6. Transfer Curve illustrating INL error [2]

- Differential Nonlinearity Error(DNL): Differential nonlinearity error is difference between the actual code width of a non-ideal converter and the ideal converter. Figure 6 illustrates the DNL error.

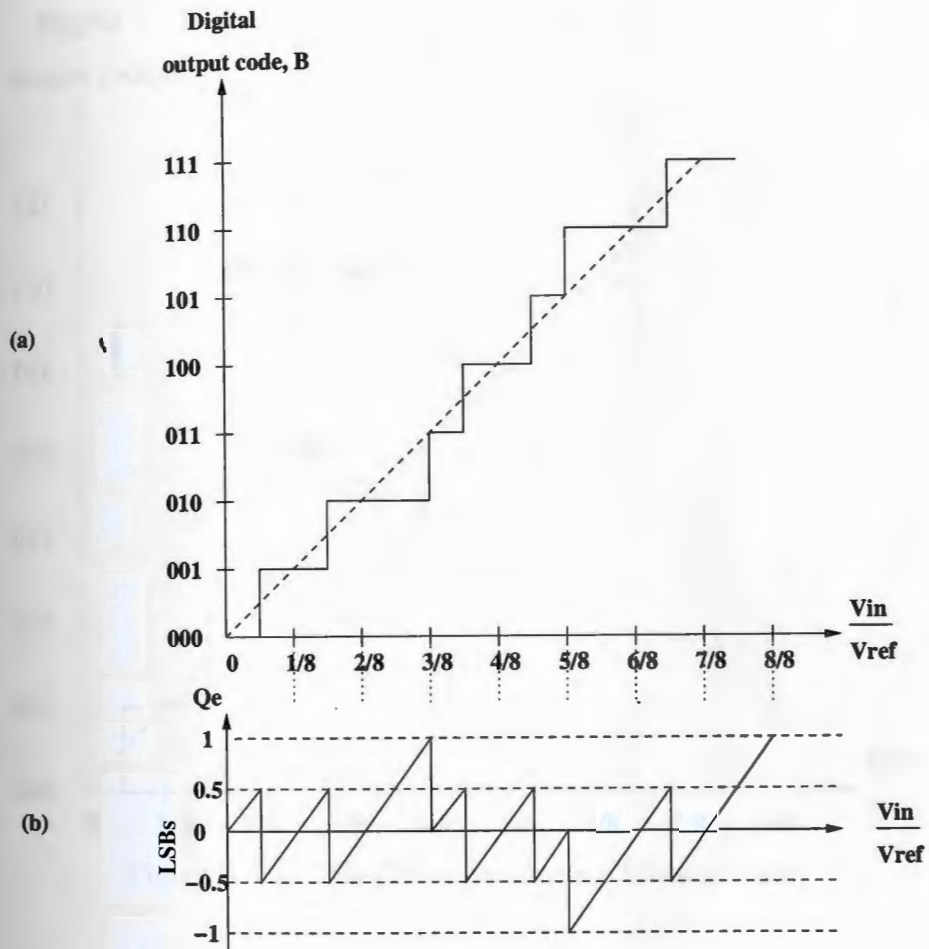


Figure 7. Transfer Curve illustrating DNL error [2]

- Missing codes: When no value of input voltage will produce a given output code, that code is missing from the transfer function and is called the missing code.

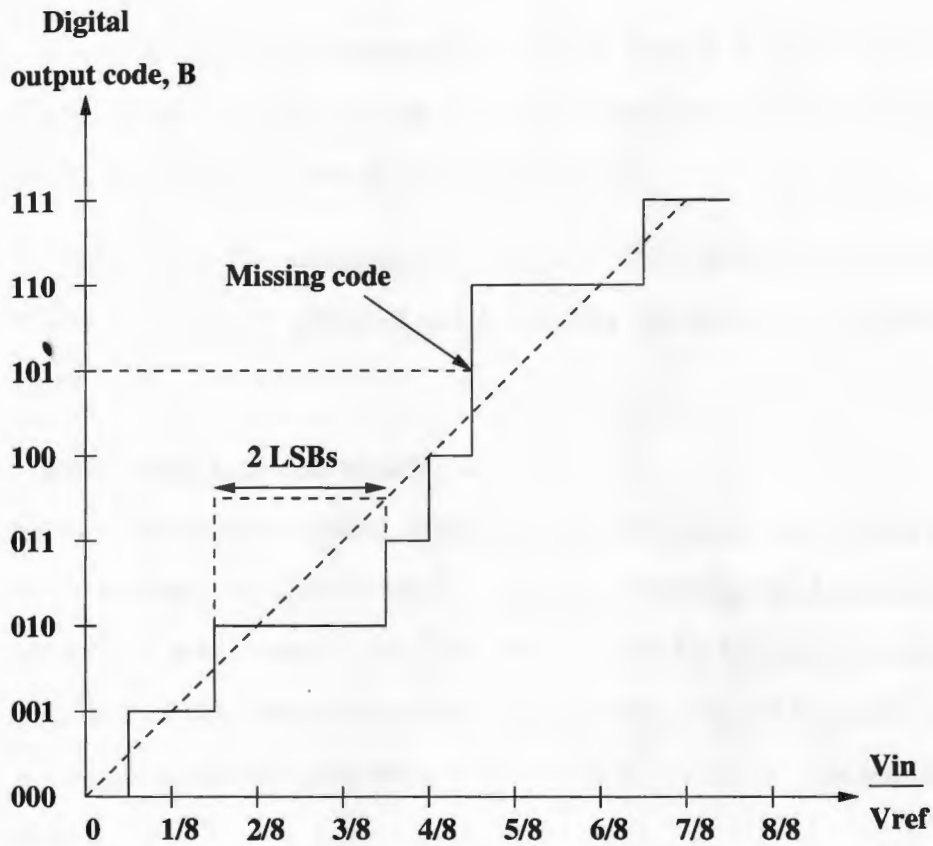


Figure 8. Transfer Curve illustrating Missing Codes

### 2.2.2 Dynamic Performance Measures

- Dynamic Range: Dynamic Range is the ratio of the maximum output signal to the smallest output signal the converter can produce (1 LSB)[3]. Dynamic range can be written as shown in the following equation.

$$DynamicRange = 20 \log_{10}(ratio) \dots (5)$$



An N-bit converter has a ratio approximately equal to  $2^N$ , then the Dynamic range is given by

$$20\log_{10}(2^N) = 20N\log_{10}2 = 6.02N(\text{dB}) \quad \dots (6)$$

- Conversion time: The conversion time of an Analog to Digital Converter (ADC), is the time taken for the converter to complete a single measurement including acquisition time of the input signal [1].
- Sampling rate: The maximum sampling rate is the speed at which samples can be continuously converted and is typically the inverse of the conversion time.

### 2.2.3 Frequency Domain Measures

- Signal to Noise Ratio (SNR): Signal to Noise ratio is the ratio of the power of the fundamental and the total noise power excluding the harmonic components. It is expressed in dB. The SNR accounts for the noise in the entire Nyquist interval. The SNR can depend on the frequency of the input signal. It usually diminishes proportional to the input. It can be mathematically written as

$$SNR = 10\log\left(\frac{\text{Signal Power}}{\text{Total noise floor power}}\right) \quad \dots (7)$$

- Signal to Noise plus Distortion (SNDR): SNDR is the ratio of the fundamental and the total noise plus harmonic power. It is expressed in dB. Mathematically, it can be written as

$$SNDR = 10\log\left(\frac{\text{Signal Power}}{\text{noise} + \text{harmonic power}}\right) \quad \dots (8)$$

- **Effective Number of Bits (ENOB):** ENOB measures the maximum signal to noise plus distortion ratio using bits. The relation between SNDR in dB and ENOB is

$$ENOB = \frac{SINAD_{dB} - 1.76}{6.02} \dots\dots (9)$$

- **Total Harmonic Distortion (THD):** THD is the ratio of the power of the fundamental and total harmonic distortion power. It is expressed in dB.

$$THD = 10\log\left(\frac{Signal\ Power}{noise + total\ harmonic\ power}\right) \dots\dots (10)$$

- **Spurious Free Dynamic Range (SFDR):** SFDR is the ratio of the power of the signal and the power of the largest spurious frequency components. The SFDR is usually expressed in dB. Mathematically, it can be written as

$$SFDR = 10\log\left(\frac{Signal\ Power}{power\ of\ the\ largest\ spurious\ frequency}\right) \dots\dots (11)$$

The figure illustrates the SFDR and other frequency domain parameters.

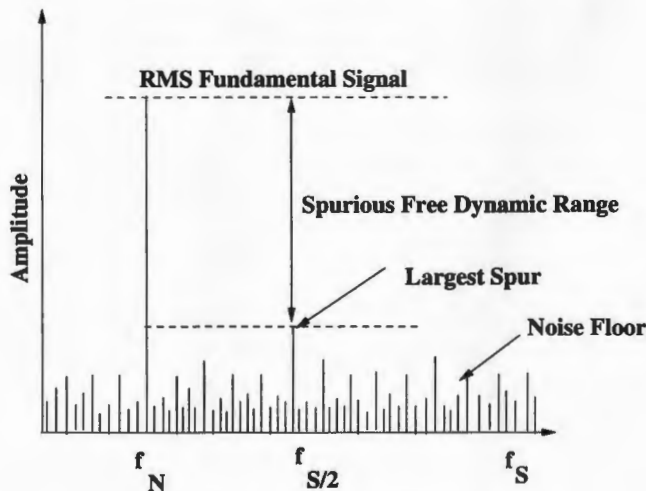


Figure 9. SFDR Illustration

## List of References

- [1] K. M. David A. Johns, *Analog Integrated Circuit Design*. New York, United States of America: John Wiley and Sons, 1997.
- [2] D. B. R.J Baker, Harry W. Li, *CMOS circuit Design, Layout and Simulation*. New York, United States of America: IEEE Press Series on Microelectronic Systems, 1998.
- [3] E. Cliffs, *Devices, Analog-Digital Conversion Handbook*. New Jersey, United States of America: Prentice Hall, 1996.

## CHAPTER 3

### ADC Architectures

This chapter discusses various architectures available for designing Analog to Digital Converters and the comparison of different performance measures and trade offs of different architectures.

Data converters are broadly classified as Nyquist-Rate Converters and Oversampling Converters depending on the Sampling rate. Oversampling Converters categorizes data converters with a large Oversampling Ratio, whereas the Nyquist-Rate converters have a small Oversampling Ratio. The ratio between the Sampling rate  $f_s$  and twice the Signal bandwidth is defined as the Oversampling ratio (OSR).

$$OSR = f_s/2f_b \quad \dots\dots (12)$$

The basic idea of this thesis is to design and implement a Successive Approximation ADC, hence popular Successive Approximation ADC architectures are discussed in the second part of the chapter.

#### 3.1 Different ADC Architectures

As already mentioned, Data converters are classified into two main categories, Nyquist rate data converters and Over sampling data converters based on the sampling rate. Flash ADC, Pipelined ADC, Successive Approximation ADC and Integrating ADC fall under Nyquist rate Data converters. Sigma-Delta ADCs fall under the Over sampling data converter category. Each has benefits that are unique to that architecture and span the spectrum of high speed and resolution.

##### 3.1.1 Flash ADCs

Flash ADC's, also known as the parallel ADC's, have the highest speed compared to other ADC architectures [1]. As illustrated in Figure 10 , a Flash

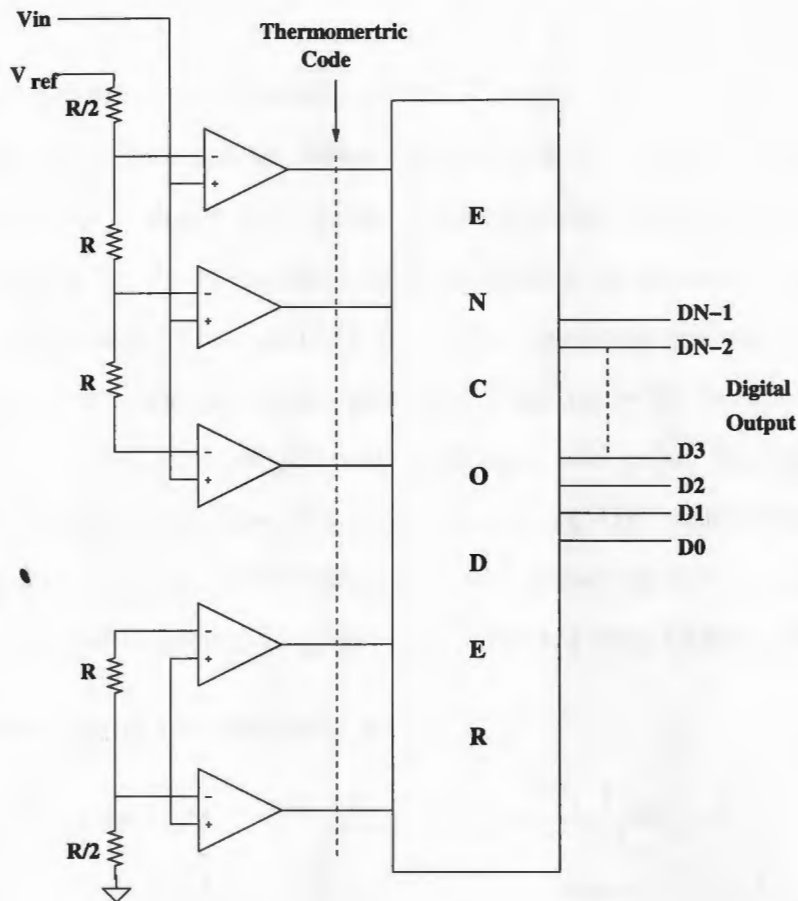


Figure 10. Flash ADC

ADC consists of one comparator per quantization level, i.e.  $(2^N - 1)$  comparators, and a resistor string DAC consisting of  $2^N$  resistors, where  $N$  represents the number of bits or the resolution of the ADC. The reference voltage is divided into  $2^N$  reference values by the DAC resistor string, these reference values are individually compared to the input voltage via a set of comparators resulting in a thermometer code. Thus, the comparator outputs simultaneously present  $(2^N - 1)$  discrete digital states. The thermometric code consists of all zeros for each resistor level if the reference value is less than the input voltage and all ones, if the reference value is greater than or equals the input voltage. The thermometric code is converted into a digital word by using a corresponding encoder.

### Design considerations and implications

The Flash architecture has the advantage of being very fast, because the conversion occurs in a single ADC cycle. The advantage of having high speed is counterbalanced by the requirement of large number of comparators that need to be carefully matched and properly biased to ensure that the results are linear [2]. Since the number of comparators needed for an  $n$ -bit resolution ADC is equal to  $(2^N - 1)$ , limits of physical integration and input loading keep the maximum resolution fairly low. For example, a 16-bit ADC would require 65,535 comparators; hence Flash ADC's have traditionally been limited to a maximum of 8-bit resolution with conversion speeds of 10 - 40 Ms/s using CMOS technology[2].

#### 3.1.2 Subranging or Two-Step ADCs

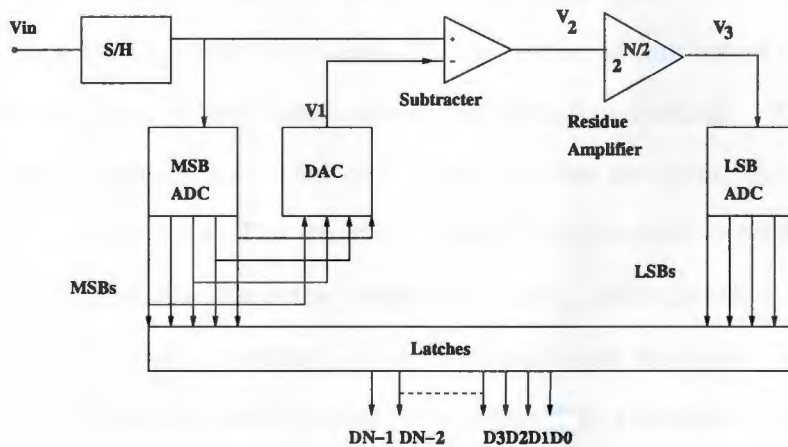


Figure 11. subranging converters

A Two-Step Flash Converter, also known as a Subranging Converter, overcomes few of the limitations of a Flash Converter. Figure 11 illustrates the basic block diagram of a Two-Step Flash Converter. The Converter essentially consists of two Flash ADC's separated using a feed forward circuitry. The first converter generates a rough estimate of the value of the input, and the second

converter refines the conversion. The input is first sampled and the first Flash ADC determines the Most Significant Bits (MSBs). The quantization error is calculated by reconvertng the MSBs to an analog value with a DAC and subtracting that value from the input signal. The residue of the subtraction is then multiplied by  $2^{N/2}$  and input into the second Flash ADC. The multiplication allows the two ADCs to be identical and also increases the strength of the signal fed to the second Flash ADC. The LSBs are then determined by the second Flash ADC.

#### *Design considerations and implications:*

Two-Step Converters are popular as high-speed, medium accuracy ADCs. These Converters have several advantages over the Flash ADCs. Specifically, the number of comparators is greatly reduced from  $(2^N - 1)$  to  $2(2^{N/2} - 1)$  comparators, thus the silicon area is greatly reduced. The reduction in number of comparators greatly reduces total power dissipation and capacitive loading. The voltages required by comparators to resolve the output are less stringent when compared to the Flash counterparts. The tradeoff is that the conversion process is done in two steps instead of one, thus the latency increases, although their throughput approaches that of flash converters, if the two stages are pipelined. The speed is limited by the band-width and settling time required by the residue amplifier and the summer [1].

### **3.1.3 Pipelined ADCs**

The Pipelined Converter is an improvement on the Subranging Converter as it divides the conversion task into several consecutive stages. As illustrated in Figure 12 , each of these stages consists of a sample-and-hold circuit, an m-bit ADC, for example a Flash Converter, and an m-bit DAC. First the sample-and-

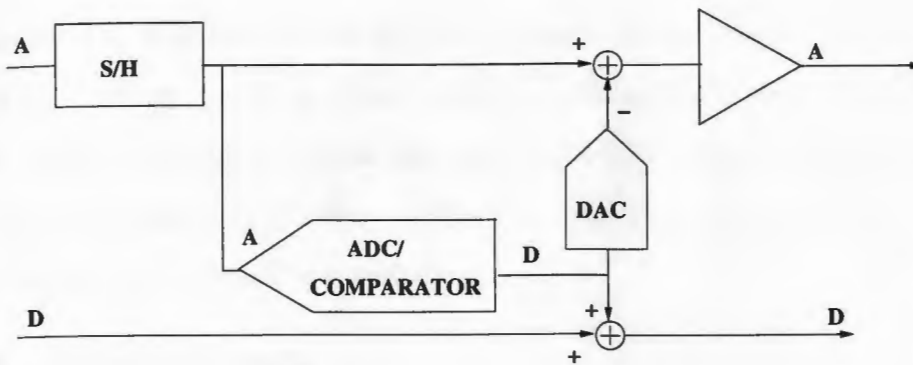


Figure 12. Pipelined Converters

hold circuit of the first stage acquires the signal. The  $m$ -bit Flash Converter then converts the sampled signal to digital data. The conversion result forms the Most Significant Bits (MSBs) of the digital output. This same digital output is fed into an  $m$ -bit Digital to Analog Converter (DAC), and its output is subtracted from the original sampled signal. The residual analog signal is then amplified and sent onto the next stage in the pipeline to be sampled and converted as it was in the first stage. This process is repeated through as many stages as are necessary to achieve the desired resolution. In principle, a pipelined converter with ' $p$ ' pipeline stages, each with an  $m$ -bit Flash Converter, can produce a high speed ADC with a resolution of  $N = p \times m$  bits using  $p \times (2^m - 1)$  comparators. For example, a two stage pipelined converter with 8-bit resolution requires 30 comparators.

#### *Design Consideration and Implications*

Pipelined Converters achieve higher resolutions when compared to the Subranging Converters and the Flash Converters containing a similar number of comparators. This comes with a price of increasing the total conversion time from one cycle to ' $p$ ' cycles. But since each stage samples and hold its input, ' $p$ ' conversions can be underway simultaneously. The total throughput can therefore be equal to the throughput of a Flash or a Subranging Converter, i.e., one conversion



per cycle. The difference is that for the Pipelined Converter, the Latency is 'p' cycles [1]. Another limitation of the Pipelined architecture is that the conversion process generally requires a clock with fixed period. Converting rapidly varying non-periodic signals on a traditional Pipelined Converter can be difficult because the Pipeline typically runs at a periodic rate.

### 3.1.4 Integrating ADCs

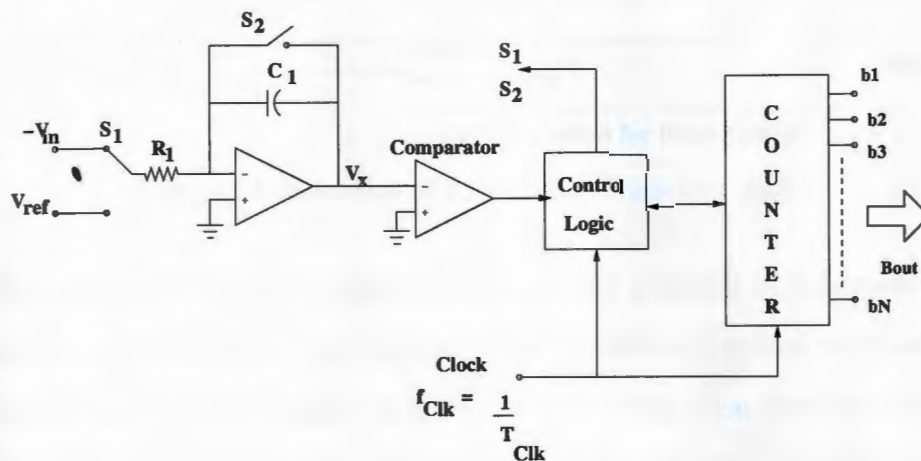


Figure 13. Integrating Converter ADC

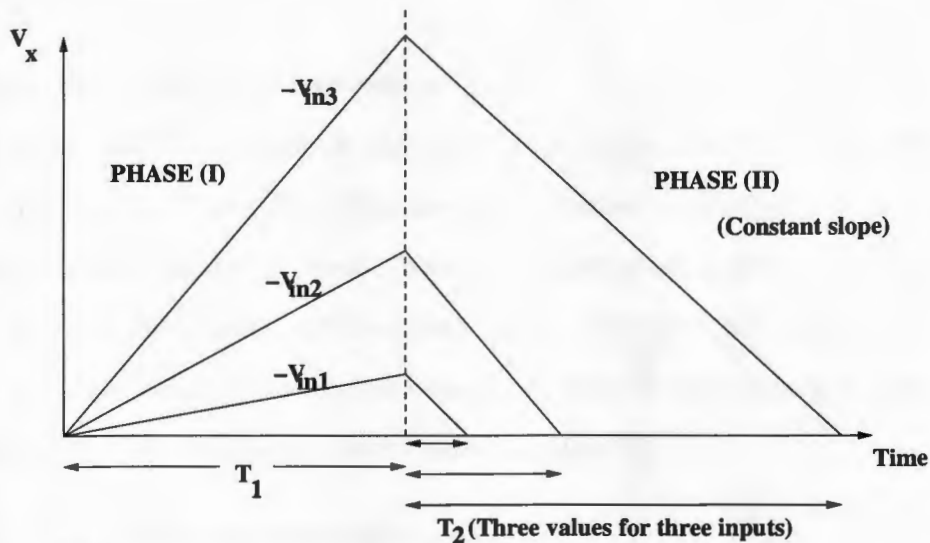


Figure 14. Behavior of Integrating Converter ADC

Integrating ADCs are a popular approach for realizing high-accuracy data conversion on very slow-moving signals. These converters perform the conversion by integrating the input signal and correlating the integration time with a digital counter. Figure 13 illustrates the basic block diagram of a Dual-Slope ADC. Dual-Slope refers to this converter since it performs its conversion in two phases. In phase I, the integration is performed on the input signal and in phase II, the integration is performed on the reference signal. The input voltage in this case is assumed to be negative, so that the output of the inverting integrator results in a positive slope during the first integration. Figure 14 illustrates the behavior of the Dual-Slop Converter. The first integration is of fixed length, which is decided by the counter. The sampled signal produces a varying slope. After the counter is reset, the reference voltage is connected to the input of the integrator. The inverting integrator output will start to discharge down to zero at a constant slope as the input is negative with respect to the reference voltage. The counter again counts the time taken by the integrator to discharge. The final count is equal to digital value of the input.

### *Design Consideration and Implications*

Integrating ADC's are used in high resolution applications but have relatively slow conversions. These Converters have comparatively low offset and gain errors in addition to being highly linear. Another advantage of these Converters is that they have a simple circuit implementation and occupy little silicon area. They are very inexpensive to produce and are commonly used in slow-moving and low cost applications like voltage and current meter displays [2].

#### 3.1.5 Successive Approximation ADCs

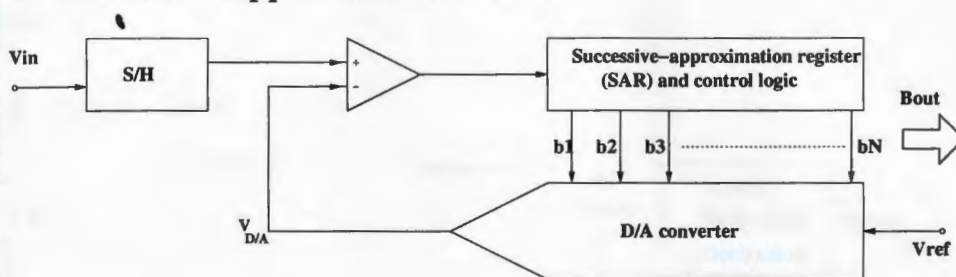


Figure 15. Successive Approximation

Successive Approximation ADCs (SAR) have a reasonably good resolution with quick conversion time. These can be thought of as being orthogonal to the Flash architecture. While a Flash ADC uses many comparators to convert in a single cycle; an SAR converter, as shown in Figure 15, conceptually uses a single comparator over many cycles to make its conversion. The SAR converter basically performs a binary search through all possible quantization levels before converging on the final digital output. To elaborate its operation, in the first cycle, the Most Significant Bit (MSB),  $b_1$ , is determined. In the second cycle, the next bit,  $b_2$ , is determined followed by the remaining bits until the N bits of the ADC are determined. Thus, a straight forward implementation application of an SAR ADC requires N clock cycles to complete the conversion.

### *Design Consideration and Implications*

An SAR converter can use a single converter to realize a high resolution ADC, but requires  $N$  comparison cycles to achieve  $N$ -bit resolution, compared to 'p' cycles for a Pipelined Converter and one cycle for a Flash Converter. SAR Converters have a relatively simple design and are generally used for low speed and higher resolution applications. SAR converters are also well suited for applications that have non-periodic inputs, since conversions can be started at will. This feature makes the SAR architecture ideal for converting a series of time-independent signals.

#### 3.1.6 Sigma-Delta ADCs

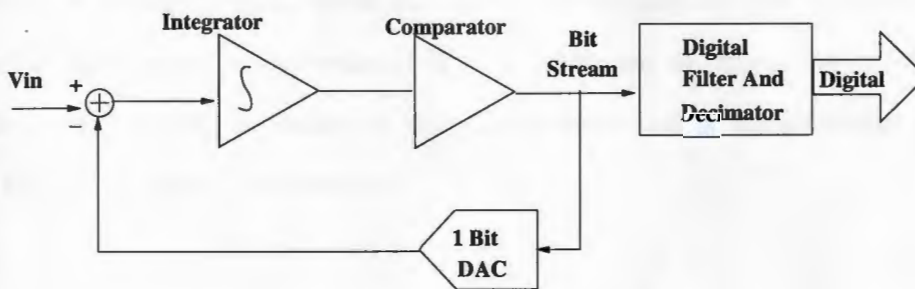


Figure 16. Sigma-Delta Converter

Sigma-Delta Converters fall under the Oversampling Converters. As already mentioned, these converters are sampled at sampling rates much higher than the Nyquist rate. In its basic form, a Sigma-Delta Converter consists of an Integrator, a Comparator, and a single bit DAC as illustrated in Figure 16. The output of the DAC is subtracted from the input signal. The resulting signal is then integrated, and the integrator output voltage is converted to a single-bit digital output (1 or 0) by the comparator. The resulting bit becomes the input to the DAC, and the DAC's output is subtracted from the ADC input signal. This closed-loop process is carried out at a very high "Oversampled" rate. The digital data coming

from the ADC is a stream of "ones" and "zeros," and the value of the signal is proportional to the density of digital "ones" coming from the comparator. This bit stream data is then digitally filtered and decimated to result in a binary-format output.

### *Design Consideration and Implications*

One of the most advantageous features of Sigma-Delta architecture is the capability of noise shaping, a phenomenon by which much of the low-frequency noise is effectively pushed up to higher frequencies and out of the band of interest [2]. As a result, the Sigma-Delta architecture has been very popular for designing low-bandwidth high-resolution ADCs for precision measurement. Another advantage is that, since the input is oversampled, the requirement of anti-alias filtering is greatly relaxed [1]. A limitation of this architecture is its latency. The latency is caused by the digital filter and is substantially greater than that of the other architectures.

### 3.2 Comparison of Different Architectures

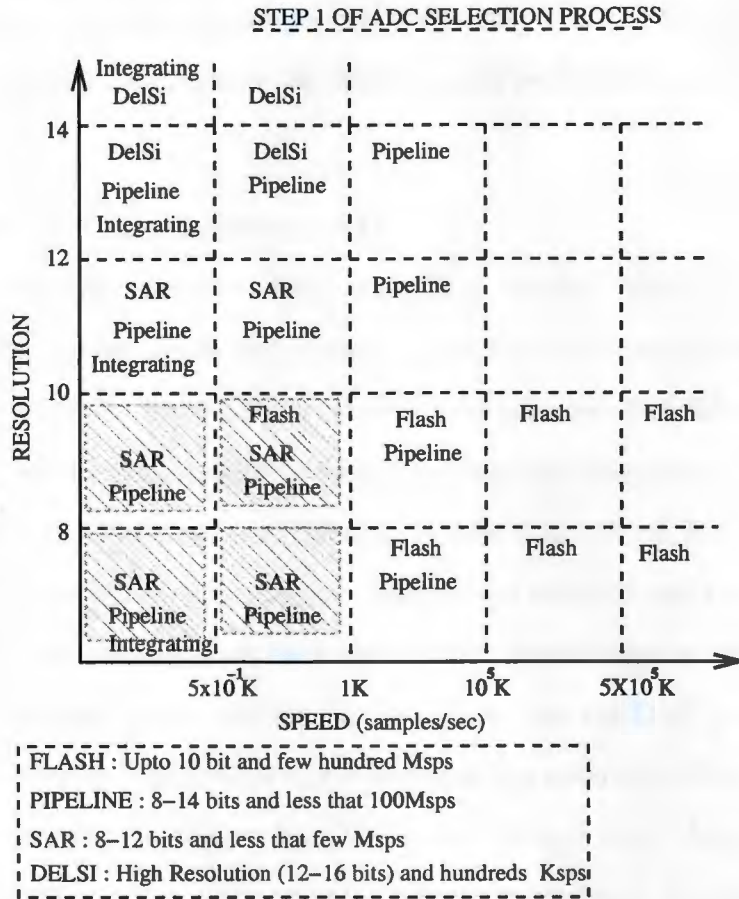


Figure 17. Comparison of Different ADC architectures.

Figure 17 compares the different architectures of ADC based on the speed of operation and the resolution that can be achieved. As already discussed, Flash ADC have the highest speed but at a low resolution due to the increase in the implementation costs with the increase in resolution. Pipelined Converters come next to the flash ADC's in conversion time with a reasonably good resolution. SAR's are popular for reasonably quick conversion time yet moderate circuit complexity. They are also known to have good resolution. Sigma-Delta's that fall under over-sampling converter architecture have a very good resolution at reasonably high speeds. Thus, depending on the application a particular architecture is a "best

choice" specific to that application and as discussed in the previous section, every architecture has its own advantages and trade-offs. Hence the designer depending upon the application, selects the most suitable architecture for that particular design.

### 3.3 Successive Approximation ADC

Successive Approximation ADC employs a "binary search" algorithm in a feedback loop to determine the closest digital word to match an input signal. As illustrated in the Figure 15, a Successive Approximation ADC in its most straight forward implementation consists of a front end Sample and Hold circuit, a Comparator, Control Logic and Decision register and a DAC. During the binary search, the circuit halves the difference between the sampled and held signal,  $V_{IN}$ , and the DAC output,  $V_{D/A}$ , in each clock cycle. Specifically, in the first period, the decision register is set to mid-scale (100...0) so that the DAC produces a mid-scale analog output. The comparator determines the polarity of  $V_{IN} - V_{D/A}$ . This determines the Most Significant Bit (MSB), b1. Thus, if  $V_{IN} > V_{D/A}$ , the MSB is set to 1 and if,  $V_{IN} < V_{D/A}$ , it is set to 0. In the second period, the decision register is pointed to (110...0) and the next bit b2 is determined followed by b3, and so on until all N bits are determined. Thus, in its most straightforward implementation, a successive-approximation converter requires N clock cycles to complete an N-bit conversion. A Flow Graph in the Figure 18 illustrates the signed conversion using the Successive Approximation approach.

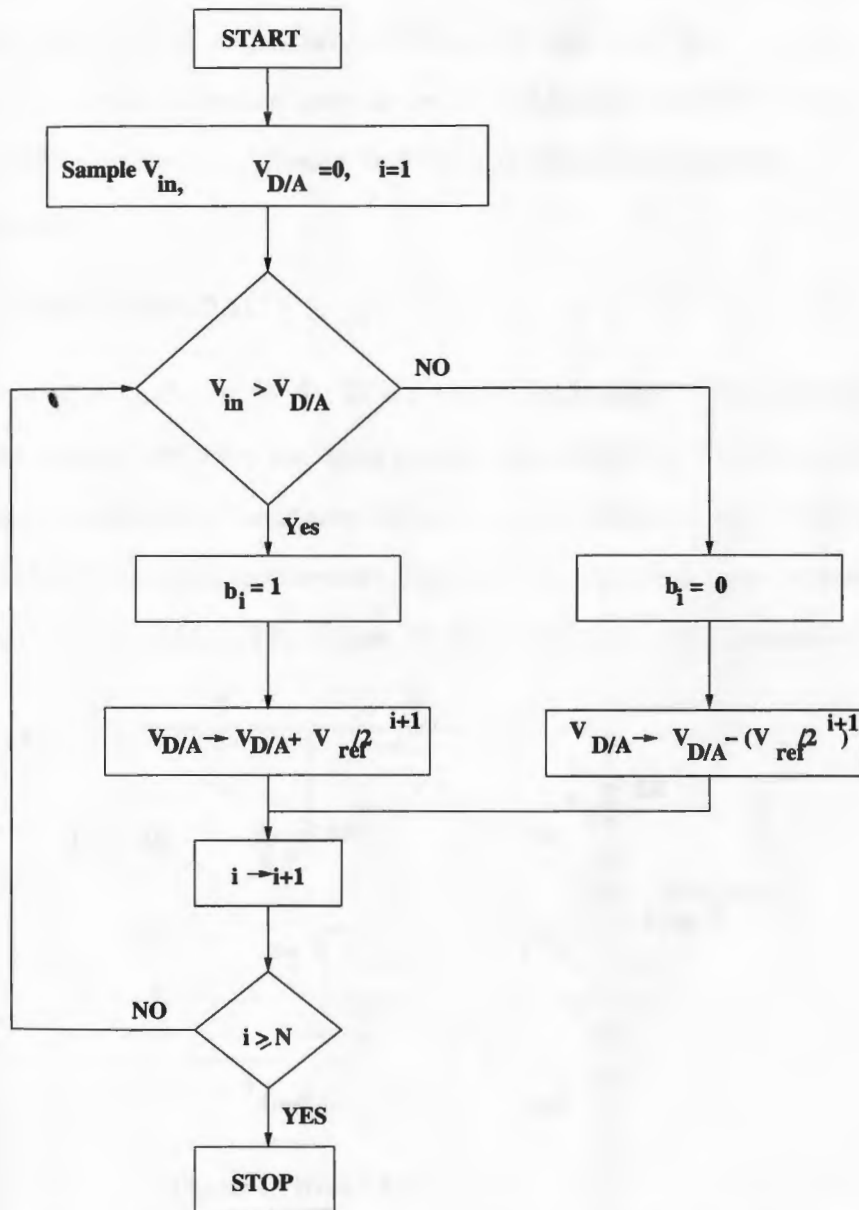


Figure 18. Flow graph illustrating binary search algorithm [2]



### 3.3.1 DAC - Based Successive Approximation ADC

A Successive Approximation ADC's performance, employing a DAC in the feedback path, depends primarily on the DAC's performance. In particular, Differential and Integral nonlinearity of the ADC are given by those of the DAC, and the maximum conversion rate of the ADC is limited by DAC's output settling time. In this section, the different DAC architectures implemented in a SAR ADC are discussed.

- **R-2R Ladder DAC :**

A very popular architecture for DACs use R-2R ladders. This architecture has the advantage of realizing the binary-weighted currents with a small number of components and with a resistance ratio of only 2, independent of the resolution of the DAC. Thus, this architecture has an advantage over conventional Binary-weighted Resistor DACs. The Figure 19 illustrates the implementation of an R-2R

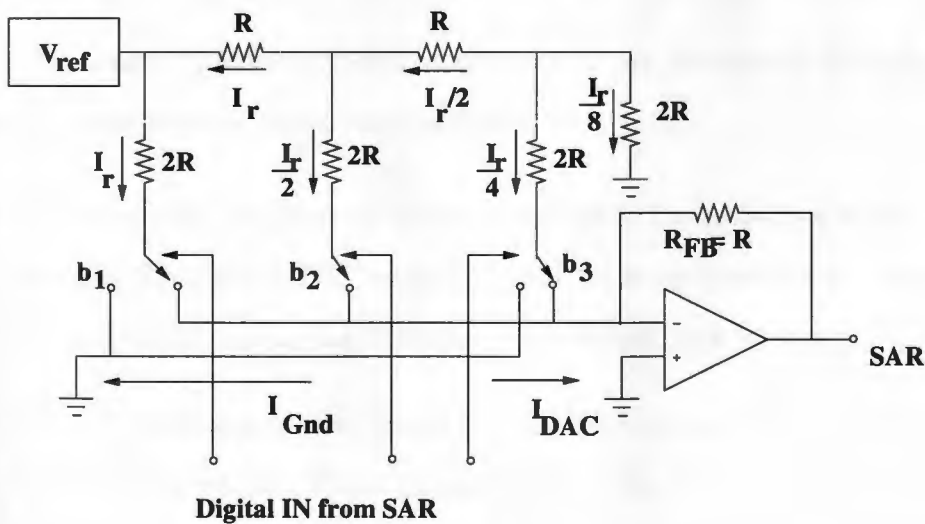


Figure 19. 3-bit R-2R ladder DAC

ladder DAC. The  $I_{DAC}$  and  $I_{GND}$  currents are maintained at ground potential, either by the Op-amp summing junction or by a direct connection to ground. The

switches steer the current either to the summing junction or to ground depending on the individual digital logic levels applied to each of the switches coming from the SAR. For example, logic "high" to  $b_1$  will cause the current,  $I_r$ , of the Most Significant Bit (MSB) to add to the  $I_{DAC}$ . For a digital "low" the same current would flow to ground  $I_{GND}$ . Since the magnitude of the MSB current is half of the full scale current it will result in an output voltage that is half of the full scale output voltage. Thus for a above architecture,

$$I_r = \frac{V_{ref}}{(2R)} \dots\dots (13)$$

And

$$V_{out} = \sum_{i=1}^N \frac{(b_i I_r)}{(2^{i-1})} = V_{ref} \left( \frac{R_f}{R} \right) \sum_{i=1}^N \left( \frac{b_i}{2^i} \right) \dots\dots (14)$$

*Design Considerations:* Although, this architecture is an improvement on the conventional binary weighted resistor DAC, it still suffers from few disadvantages.

The Integral and Differential Non-Linearity errors are introduced from the mismatches in the resistors comprising the ladder [2].

- The finite 'ON' resistance of the switches add to the resistance of the ladder network. The switch 'ON' resistance must be much less than the resistance of the resistors comprising the ladder to maintain high accuracy.
- Another drawback of this circuit is that the currents flowing through the switches vary widely. To accommodate this, the switches sizes need to be scaled so that equal voltage drops appear across them for widely varying current levels.

• Charge Redistribution DAC :

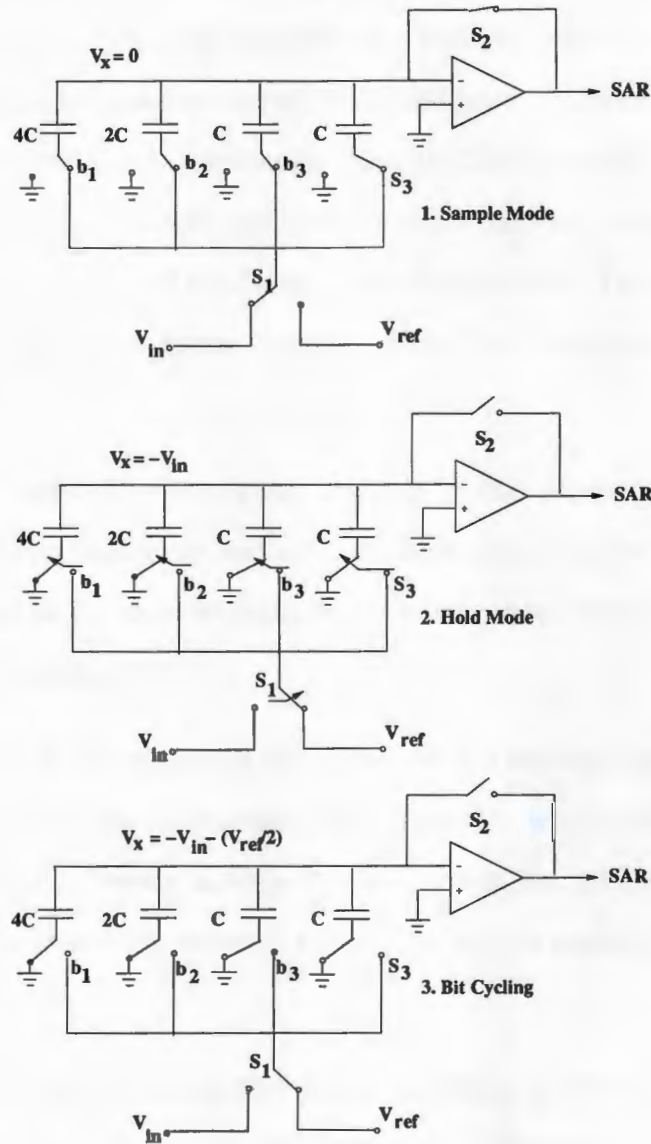


Figure 20. 3-bit charge redistribution DAC

The newer CMOS DACs implement the Charge Redistribution architecture to overcome few of the drawbacks of R-2R ladder DAC architecture. The basic idea here is to replace the input capacitor of a Switched Capacitor gain amplifier with a Programmable Capacitor Array (PCA) of binary-weighted capacitors. This approach brings the Sampling mechanism into the DAC architecture, thus the requirement for a separate Sample and Hold Circuit is removed. Figure 20 illustrates the circuit implementation of the charge redistribution DAC. This architecture operates in three stages known as the Sampling mode, Hold mode and the Bit cycling mode.

- *Sampling mode:* This forms the first step of the conversion, the capacitor array performs the sample and hold operation. In this mode all the capacitors are charged to  $V_{in}$  while the comparator is being reset to its threshold voltage through the switch S2.
- *Hold mode:* In this mode, all the capacitors are switched to ground and the comparator is taken off the reset mode. Thus,  $V_x$ , which was initially zero, is charged to  $-V_{in}$ , thereby holding the input signal,  $V_{in}$ , on the capacitor array. Finally, the switch S1 switched to  $V_{ref}$  and  $V_{ref}$  is applied to the capacitor array.
- *Bit cycling:* In this mode, the largest capacitor is switched to  $V_{ref}$ , thus charging  $V_x$  to  $(-V_{in} + V_{ref} / 2)$ . Now if  $V_x$  is negative, then  $V_{in}$  is greater than  $V_{ref} / 2$ , and the MSB capacitor is left connected to  $V_{ref}$ . Thus, the MSB bit is considered 1, or else the MSB capacitor is reconnected to ground and bit is taken to be 0. This process is repeated N times, with a smaller capacitor being switched each time, until the conversion is completed.

*Design considerations:* The main advantages of the Charge-Redistribution DAC are the higher speeds, the inherent Sample and Hold function, the increased accuracy and the smaller die size compared to the R-2R ladder architecture. Despite the advantages, this architecture suffers few disadvantages.

- For high resolutions, the ratio of the largest and the smallest capacitor is  $(2^{N-1})$ , where N is the resolution, as well as the total value of the array capacitance, can be excessively large. For example, in a 12-bit converter, the ratio of the MSB and to the LSB capacitor is equal to 2048, and the array comprises 4096 equal unit capacitors.
- The minimum size of the smallest capacitor is often dictated by uniformity and matching considerations. Hence, the area and the capacitance of large arrays are huge and this results in an enormous input capacitance for the converter, which in turn slows down the preceding circuit.
- The Layout gets complicated due to the large capacitor array.
- The large capacitance of the array draws large current spikes from the Ground and  $V_{ref}$  lines during transients, causing ringing and long settling times in the presence of inductance in series with these lines [1].
- **Charge Division by 2 circuit:**

This architecture overcomes few of the drawbacks of the Charge redistribution architecture. The proposed Divide by 2 circuit, as the name goes, divides the charge into half the original charge every clock cycle. This operation is repeated over for N consecutive cycles, where N is the resolution. Figure 21 illustrates the Divide by 2 circuit implementation. The circuit is realized using a Switched Capacitor implementation. The operation of the circuit is explained in detail below:

- *Phase I:* In this phase, switches 1a and 1 are closed as illustrated in the figure. During this phase, the first capacitor, C, gets charged to  $V_{ref}$ , while the Op-amp is being reset to its threshold by closing the switch 1a.
- *Phase II:* During this phase the switches 2 and 3a are closed. In this phase, the Op-amp is taken off the reset mode and the charge across the first Capacitor C, i.e.  $V_{ref}$ , appears at the output of the Op-amp while the second Capacitor is being discharged to ground.
- *Phase III:* During this phase the switches 1b, 1 and 3a are closed. In this phase, both capacitors fall parallel to each other. As they have the same Capacitance C across them, the total capacitance is equivalent to 2C based on the rule of equivalent capacitance across parallel capacitors. Thus the total charge across the equivalent capacitance divided by 2, which appears at the output of the Op-amp.

Phases II and III are repeated consecutively for N cycles, where N is the resolution of the ADC.

*Design Considerations:* The main advantages of the Divide by 2 circuit are the simpler circuitry and the reduced number of capacitors required when compared to the Charge Redistribution Circuitry. Despite the simple circuitry, one has to take into consideration the non-linearity introduced due to the following inherent characteristics of a switched capacitor circuits:

- *Capacitor Mismatch:* Capacitor Matching forms the most important criteria in this architecture as the division of charge has to be precise to guarantee linearity of the division by 2 circuit. Hence the capacitors have to be matched accurately. Ideally the capacitor size is given by

$$C = (\epsilon_{ox}/t_{ox})A = C_{ox}.W.L \quad \dots (15)$$

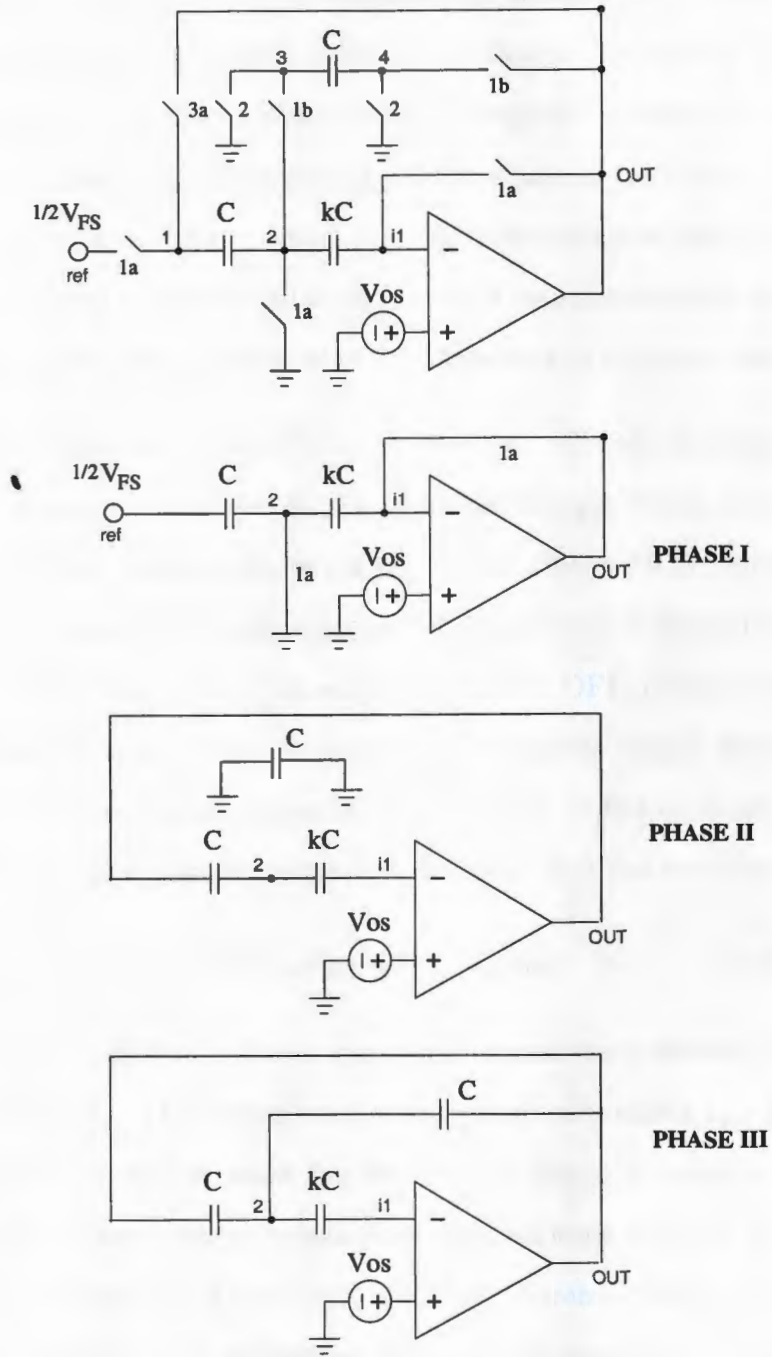


Figure 21. The working of charge division by 2 circuit

The mismatch in the capacitors arises from both the oxide thickness gradient across the surface of the microcircuit and the random variations in length and width of the capacitor which occurs due to overetching. The error introduced due to overetching is usually dominant and can be minimized by realizing larger capacitors from a parallel combination of smaller, unit-sized capacitors. Errors due to gradient of the oxide thickness can be minimized by interspersing the unit-sized capacitors in a common-centroid layout so that the gradient changes affect both the capacitors in the same way.

- *Charge Injection or the Clock Feedthrough:* Charge injection or Charge Feedthrough error is due to the unwanted charges being injected into the circuit when the transistors are turned off. When MOS switches are ON, they operate in the triode region and have zero volts between their drain and the source. When MOS transistors are turned OFF, charge errors occur by two mechanisms. The first is due to the channel charge, which must flow out from the channel region of the transistor to the drain and the source junctions. The channel charge of a transistor that has zero  $V_{DS}$  is given by

$$Q_{CH} = WLC_{ox}V_{eff} = WLC_{ox}(V_{GS} - V_t) \quad \dots\dots (16)$$

The second charge is due to the overlap capacitance between the gate and the junctions. The former error usually dominates unless  $V_{eff}$  is very small. The simplest way to make the error due to charge injection small is to use large capacitors, but large capacitors require a large silicon area. An effective way to minimize this error is to use fully differential design techniques, but the tradeoff in using differential circuits is the increase in the complexity of design.



- *Offset Voltage of the Op-amp:* Input offset voltage of the Op-amp is a source of error. The input offset error might be caused by device mismatches or might be inherent in the design of the Op-amp. In Switched Capacitor applications, this offset voltage can be cancelled by realizing an extra capacitor at the input of the Op-amp.

### List of References

- [1] B. Razavi, *Data Conversion System Design*. New York, United States of America: IEEE Press, 1995.
- [2] K. M. David A. Johns, *Analog Integrated Circuit Design*. New York, United States of America: John Wiley and Sons, 1997.

## CHAPTER 4

### Design and Implementation of SAR ADC

This chapter presents the implemented ADC architecture. The various building blocks of the implemented ADC are discussed in detail with the simulation results. The control circuitry and the timing signals required for the proper functioning of the circuit are also presented.

#### 4.1 Implemented Architecture of SAR ADC

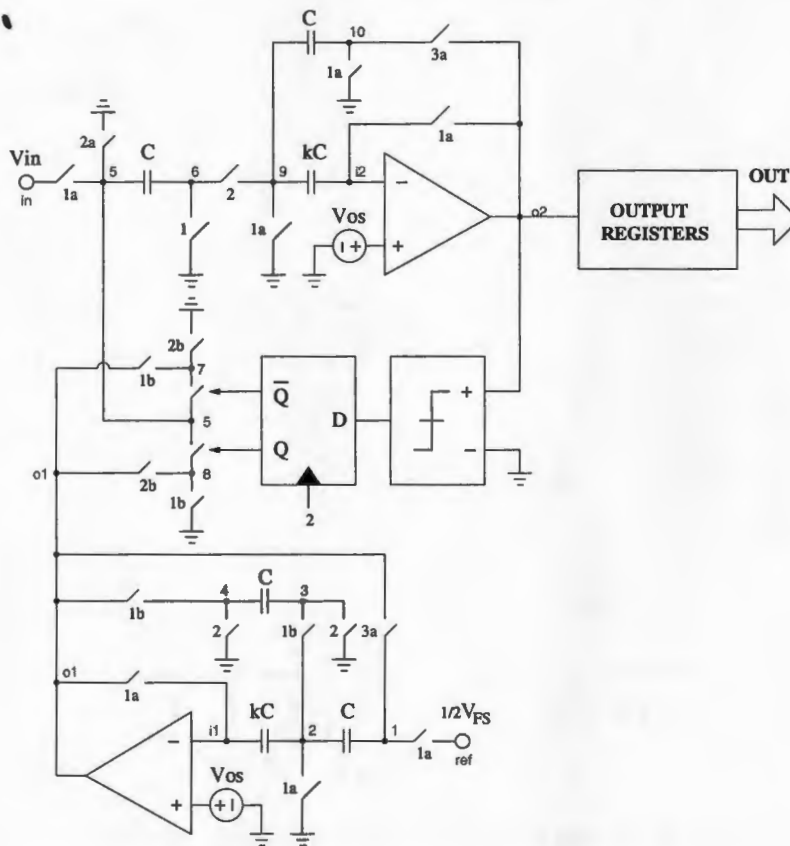


Figure 22. The implemented architecture of the SAR ADC

As already mentioned, switched capacitor techniques are used for the realization of the proposed architecture. Accuracy, simple circuit realization, good

linearity and dynamic range are few of the reasons for the popularity of switched capacitor circuitry in last few decades. The basic building blocks of a switched capacitor circuit are op-amps, capacitors, switches and non-overlapping clocks. The primary advantages of the switched capacitor implementation include compatibility with CMOS technology, good accuracy of time constants, good voltage linearity and good temperature characteristics. Despite the advantages of the switched capacitor circuits, there are few draw-backs. Clock feed-through and requirement of non-overlapping clocks fall under disadvantages of switched capacitor circuits.

The implemented architecture is shown in the Figure 22. As illustrated in this

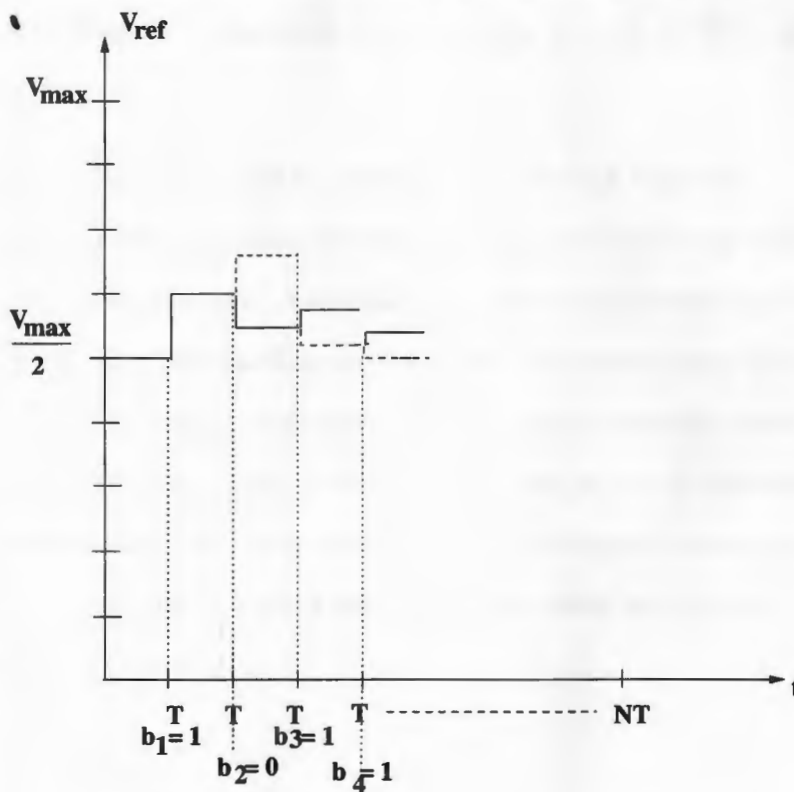


Figure 23. The conversion process of the SAR ADC

figure, the proposed architecture consists of three main blocks: An Accumulator, a Comparator and a Divide by 2 circuit. As already discussed in chapter 3, the Successive Approximation ADC's apply the binary search algorithm to determine

the closest digital word to match an input signal. The proposed architecture implements the binary search algorithm by dividing the charge into half the original charge every clock cycle. The accumulator, then depending on the previous cycle's comparator output, either accumulates or subtracts the residual charge from the original charge; if the previous cycle's comparator output equals '1', the charge gets accumulated to the original charge and if the output equals '0', the charge gets subtracted from the original charge. The output of the accumulator is then fed into the comparator, which determines the digital equivalent of the analog input. This process is repeated for  $N$  consecutive cycles, where  $N$  is the resolution of the ADC. The Figure 23 illustrates the conversion process of the proposed ADC architecture.

#### **4.2 Control Circuitry and Generation of Timing Signals**

In this section the control circuitry required for the functioning of the proposed ADC architecture is presented. As already mentioned in the preceding section, non-overlapping nature of the clocks is very critical for the functioning of the switched capacitor circuits. These clocks determine when charge transfers occur and they must be non-overlapping in order to guarantee charge is not inadvertently lost. The term non-overlapping clocks refers to two logic signals running at the same frequency and arranged in such a way that at no time both signals are high as illustrated in the Figure 24.

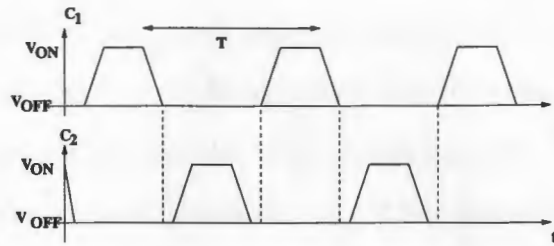


Figure 24. The non-overlapping nature of the clocks

Figure 25 illustrates the implemented control circuitry for the generation of non-overlapping clocks.

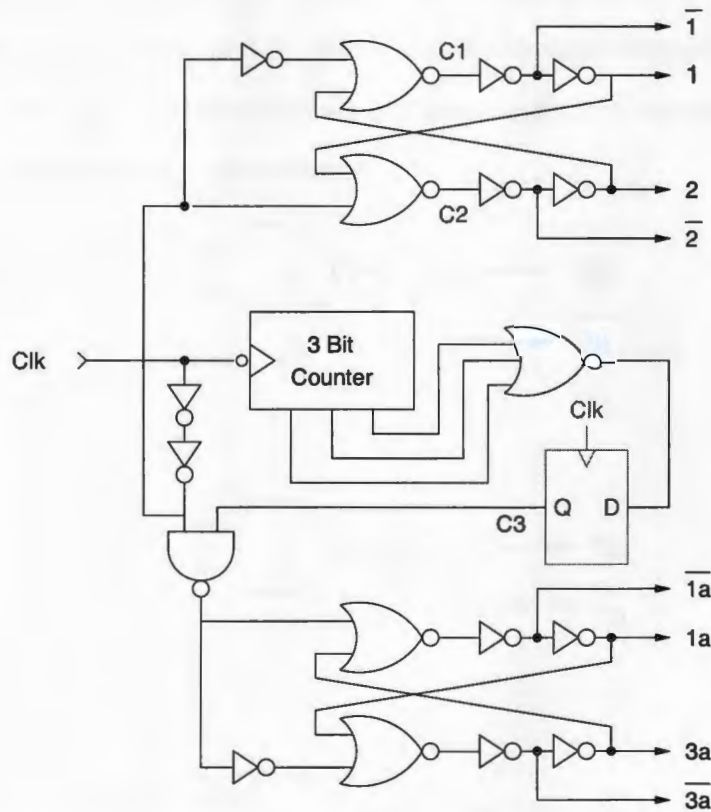


Figure 25. The control circuitry for the generation of non-overlapping clock signals

The control circuitry illustrated generates four sets of non-overlapping clocks using a master clock signal CLK. Even numbers of inverters are implemented to introduce a delay, which ensures the non-overlapping nature of the clocks. The asynchronous three bit counter is realized using T flip-flops. To realize the counter, the flip-flops are connected in cascade; with the first T flip-flop triggered by the master clock CLK and the remaining are triggered by the previous flip-flop's output. The term asynchronous is used as all the flip-flops are not triggered using the master clock CLK. The non-overlapping clocks, thus generated are used for the generation of timing signals required for the functioning of the SAR ADC. The combinational logic implemented for generation of the control signals is illustrated in the Figure 26. Figure 27 illustrates the simulation results of the control circuitry and the combinational logic implemented.

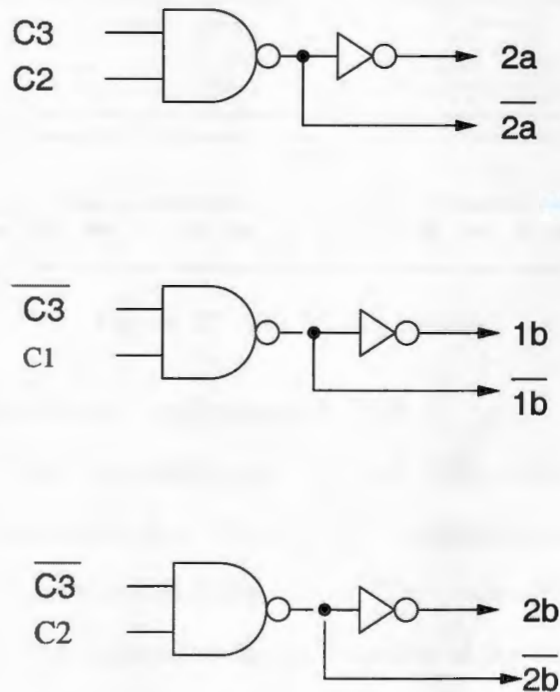


Figure 26. The combinational logic implemented to generate the timing signals

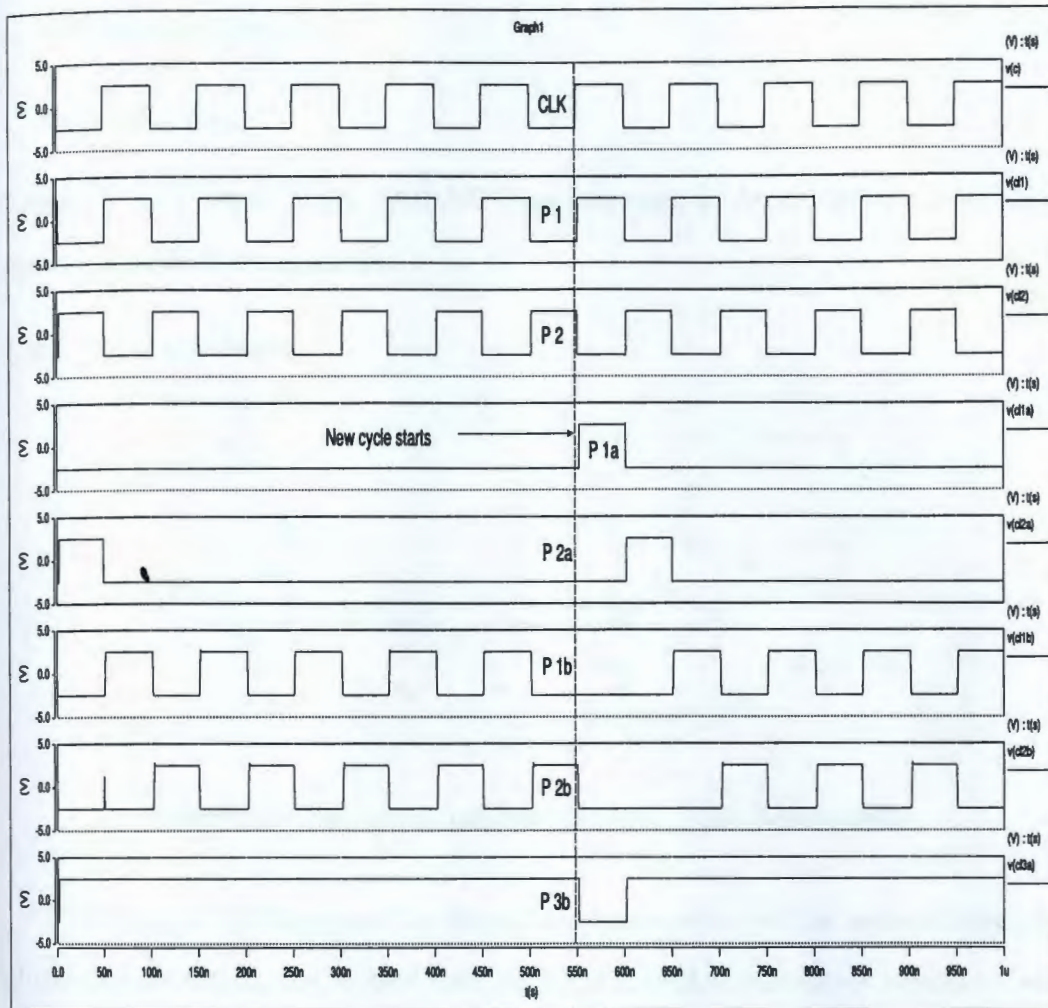


Figure 27. The timing signals

### 4.3 Main Blocks of the Implemented SAR

The design of data conversion systems deals with both architectural issues and circuit level considerations. The choice of architecture is influenced by the performance of its constituent building blocks. The trade-off's that occur at each level of abstraction often determine the performance of the complete architecture. In this section, the implementation of the main building blocks of the SAR ADC is discussed. The main building blocks of the proposed SAR ADC are

- Accumulator

- Divide by 2 circuit
- Comparator

These building blocks of the SAR ADC are discussed in detail with the simulation results in the following section.

#### 4.3.1 Accumulator

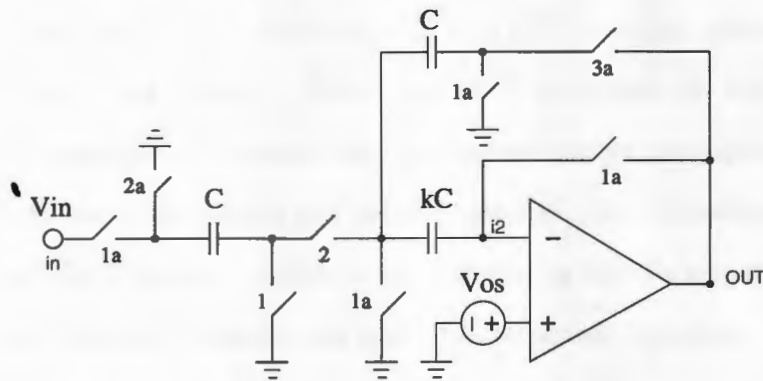


Figure 28. The circuit implementation of the Accumulator

The Figure 28 illustrates the circuit implementation of the accumulator. As illustrated in this figure, a switched capacitor based accumulator design is considered. As already discussed in the section 4.1, the accumulator based on the comparator output either accumulates the charge or substrates the charge form the input charge. Despite the simple implementation of the circuit, there are few design considerations to be taken into account when designing switched capacitor integrator circuits.

- *Implementation of the switches:* CMOS switches are implemented. The advantage of CMOS transmission gates over the conventional NMOS switches is that they have less ON-resistance. The settling behavior of the switched capacitor depends on the total capacitance and the ON-resistance of the



switches,  $\tau = C_L * R_{ON}$ , thus CMOS implementation helps in having a better op-amp settling behavior. In addition to the lesser ON-resistance, they allow a wider swing of the signals and the error introduced because of the charge injection is less in the CMOS implementation when compared to the NMOS implementation.

- *Charge Injection Error:* The MOS switches exhibit channel charge injection and clock feedthrough. When the MOS is ON, a certain amount of charge is present in its channel. When the MOS is turned off, the principle of charge conservation dictates that this channel charge gets redistributed and accumulates in the source and drain terminals. This introduces an error in the sampling capacitor, which is also referred as the clock-feedthrough. Use of large capacitors reduces the error due to charge injection. The effect of larger capacitors will be discussed in the next point.
- *Size of the Capacitors:* As already mentioned, the error due to charge injection is minimized by using larger capacitors but this is counter-balanced by increase in the total capacitance of the circuit which again has an impact total performance of the op-amp. Use of larger capacitance also increases the silicon area. Hence the size of the capacitors used has to be optimized, so that the performance of the accumulator is not affected. The size of the capacitors implemented for the proposed design is 0.8 pF, taking into account the above design considerations.
- *Op-amp offset voltage:* Finally the error introduced due to inherent op-amp offset voltage has to taken into consideration. This error at the end of the N iterations is given by

$$EC_{OS} = (1 - 2)^{-N} V_{OS} \dots\dots (17)$$

Where  $V_{OS}$  is the offset voltage of the Op-amp. This error can be minimized by implementing an extra capacitance in series with the negative input terminal of the op-amp. This capacitor then gets charged to  $V_{OS}$ , the offset voltage of the op-amp and thus cancels it out.

From the above design consideration, it can be concluded that use of larger  $(w/l)$  ratio for the switches lowers the  $R_{ON}$  of the switches and thus improves the settling behavior of the op-amp, but increases the error due to the clock-feedthrough as larger switches accumulate larger channel charges. Hence there is a trade-off in selecting the  $(w/l)$  ratio of switches. For the proposed design the size of switches implemented is  $(9/2)$ .

#### 4.3.2 Divide by 2 circuit

The Figure 29 illustrates the Divide by 2 circuit implementation. As the functionality of the divide by 2 circuit has already been in Chapter 3, it will not be dealt here to avoid redundancy. As the figure illustrates, a switched capacitor implementation is used for the design of the divide by 2 circuit also. Hence all the design considerations, discussed in case of the accumulator section, apply here. Thus, taking the various design consideration into account, the sizes of the capacitors and the switches realized is 0.8 pF and  $(w/l) = (9/2)$  respectively. The precise matching of the capacitors is very critical to achieve an accurate division of charge. Hence the error introduced due to improper matching of the capacitors should be taken into account. If it is assumed that the capacitors are matched with an error  $\epsilon$ , then the total error introduced can be calculated as follows.

From phase I, the total charge in the circuit is equivalent to

$$Q = V_{ref}C \quad \dots (18)$$

From phase II,

$$V_{out} = V_{ref}C \quad \dots (19)$$

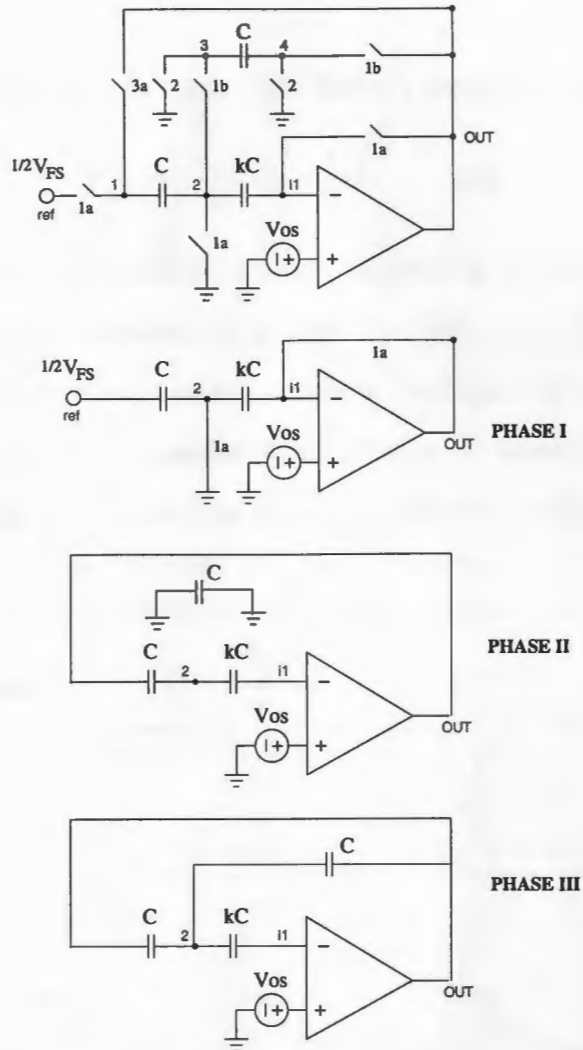


Figure 29. The divide by 2 circuit implementation

From phase III, both the capacitors are in parallel. Considering the second capacitance value is equal to  $(1 + \epsilon) C$ , the total capacitance is equivalent to  $(2 + \epsilon) C$ .

Hence

$$V_{out}(2 + \epsilon)C = V_{ref}C \quad \dots\dots (20)$$

$$\text{Thus, } V_{out} = V_{ref}/(2 + \epsilon) \quad \dots\dots (21)$$

Simplifying the about equation using the Taylor's formula, we get

$$V_{out} = \left(\frac{V_{ref}}{2}\right)\left(1 - \frac{1}{2}\epsilon\right) \dots\dots (22)$$

Repeating the above calculation of N cycles, where N is the resolution, we get the error introduced due to mismatching is given by  $\left(\frac{V_{ref}}{2^N}\right) * \left(1 - \frac{N}{2}\epsilon\right)$ .

The ways of minimizing the mismatch errors in the capacitor layout are discussed in Chapter 5 under layout considerations. Figure 30 illustrates the simulation results of the divide by 2 circuit and the accumulator implemented.

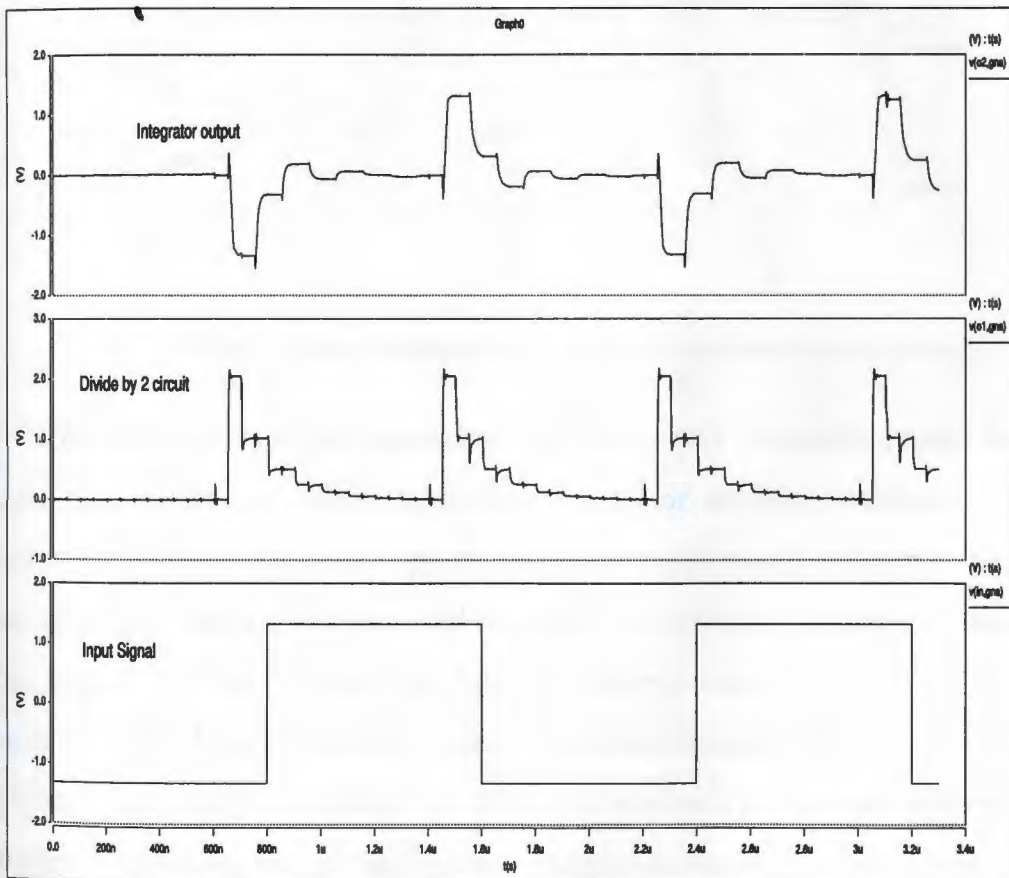


Figure 30. Simulation results of the accumulator and the divide by 2 circuit

## Op-amp

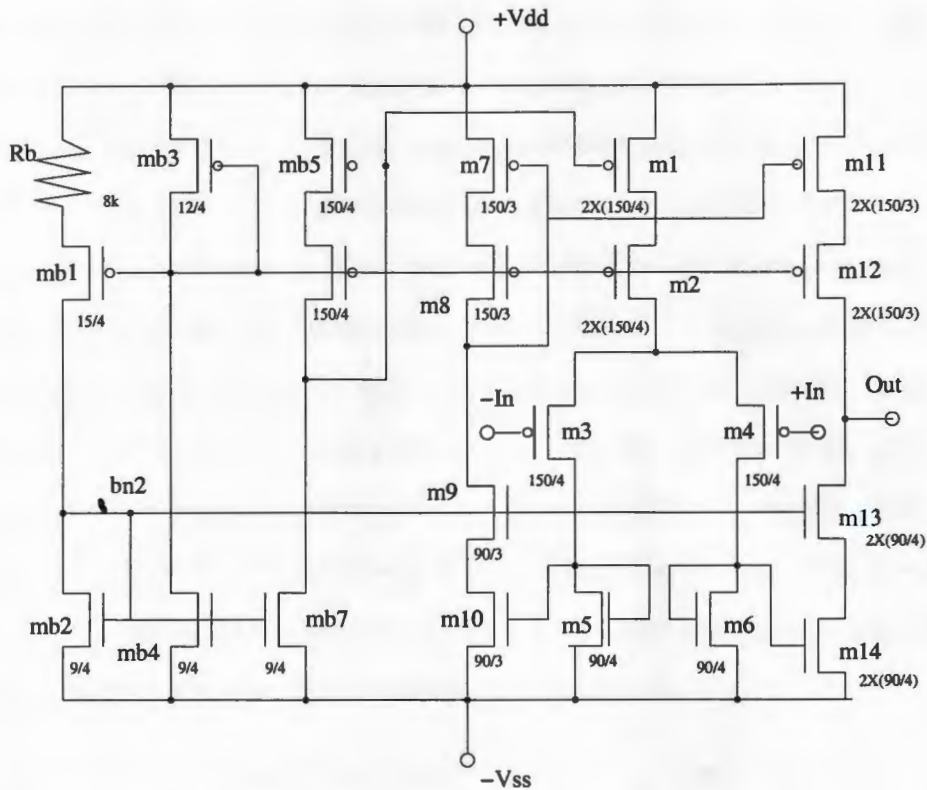


Figure 31. The circuit implementation of the transconductance op-amp

The performance of the operational amplifier is very crucial for precise functioning of the divide by 2 circuit and the accumulator and hence affects the total performance of the ADC. Although, op-amps were traditionally designed to have a gain of several hundred thousand and to provide relatively low output impedance, they have evolved into different topologies, as they are used as fundamental building in a variety of analog circuits. Various performance metrics like gain, slew rate, dynamic range and power dissipation dictate the choice of the op-amp topology to be considered for a particular application. Previous literatures show that transconductance operational amplifier is a good choice for switched capacitor circuits as the load is purely capacitive. Due to reasonably high speed and good bandwidth consideration, a current mirror transconductance op-amp configuration is selected.

Figure 31 illustrates the CMOS transconductance amplifier implemented. As the figure illustrates, the transconductance operational amplifier has three stages, the bias stage, the differential gain stage and the push pull output stage.

The settling requirements of the op-amp outputs determine unity-gain band-width (UGB) and slew rate for the given clock frequency and capacitive loads. The minimum necessary slew rate for linear settling depends on the maximum step in the op-amp output voltage and linear settling time-constant. It is a known fact that the settling time constant depends on the total capacitance of the circuit. In the case of the accumulator circuit, during the phase when the switches 2, 2a and 3a are closed the total capacitance seen by the op-amp is  $2(C/3)$ . During the phase when the switches 1b, 1 and 3a are closed, the total capacitance appearing is equal to  $C/2$ . Hence considering the worst case scenario the total capacitance that appears on the op-amp in the case of the accumulator is given by

$$C_L = 2C^2/3C = 2C/3 + C_{GS} \quad \dots\dots (23)$$

Where  $C_{GS}$  is the gate capacitance of the preceding circuitry. In case of the divide by 2 circuitry, as illustrated in Figure 28, as the circuit operates in 3 phases as discussed in chapter 3, the load capacitance in phase 2 and phase 3 is given by  $C^2/2$  and  $3C/2$  respectively. Considering the worst case scenario, the load capacitance at the output of the op-amp is given by

$$C_L = (C^2/2C) + C = 3C/2 + C_{GS} \quad \dots\dots (24)$$

As the capacitors implemented in the design of the accumulator and the divide by 2 circuit are equivalent to 0.8 pF. The op-amp required for the implementation of accumulator and the divide by 2 circuit should be able to drive a total capacitive load equivalent to at least 1.5 pF. Thus considering the worst case scenario of having a larger load capacitance on the op-amp, the op-amp to be designed has

to have the specifications of dc gain, unity gain bandwidth (UGB), phase margin and slew rate of about 70 dB, 100 MHz, 50 MHz respectively.

<b>PARAMETERS</b>	<b>VALUE</b>
$V_{DD}, V_{SS}$	+ 2.5, -2.5 respectively
DC Gain	77.102 dB
Unity-Gain Bandwidth (UGB)	104.53
Phase Margin	58 MHz
Positive Slew Rate	88.6 V/us
Negative Slew Rate	68.43 V/us

Table 1. Performance specifications

The device dimensions of the transistors considered and the architecture of the op-amp implemented are illustrated in the Figure 30. The simulation results of the designed op-amp are illustrated in the Figure 32. Table 1 lists the simulation results obtained from the designed op-amp at capacitive load of 1.5 pF. Thus, from the simulation results it can be comprehended that the designed op-amp meets the desired specifications.

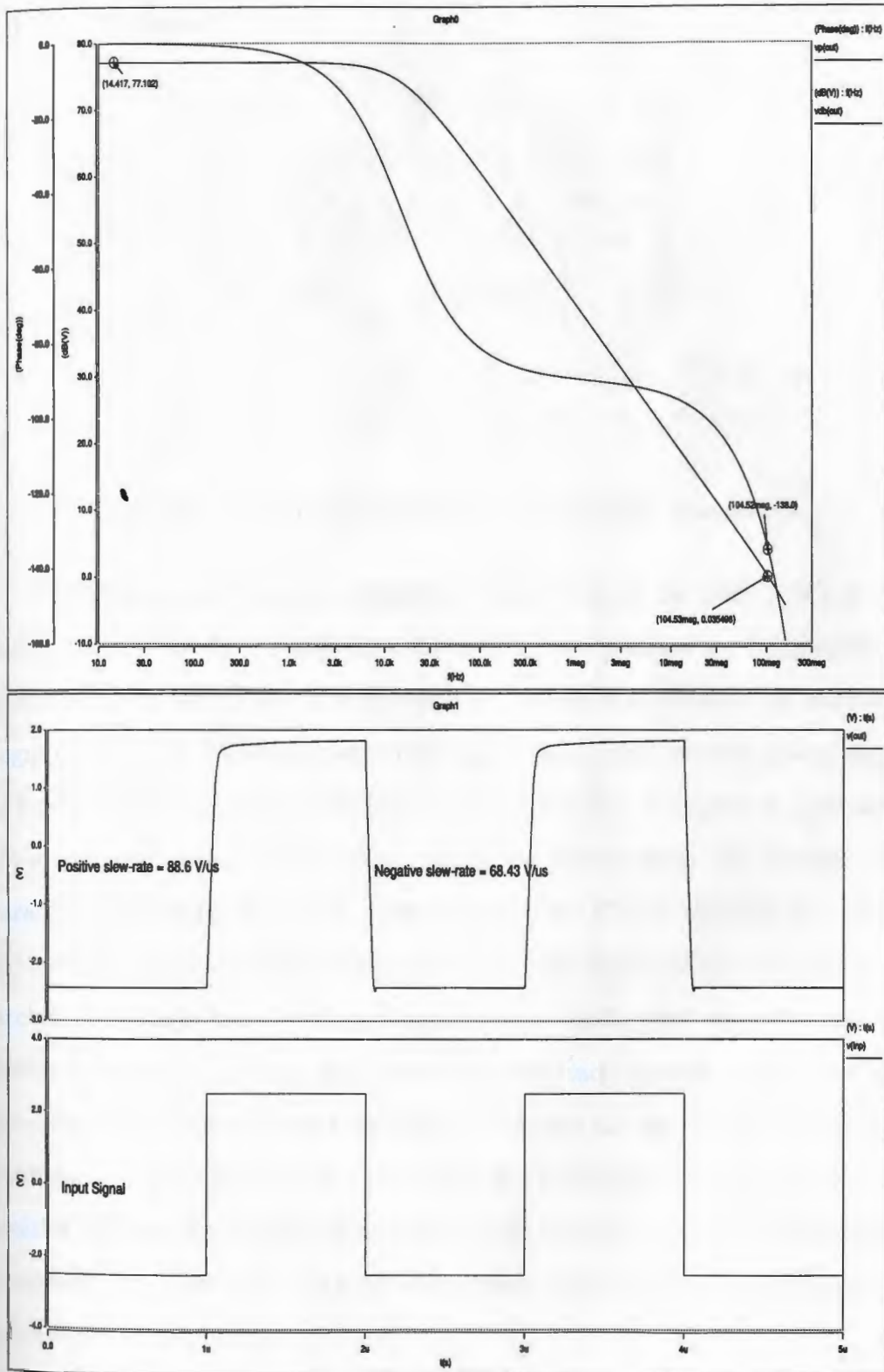


Figure 32. Simulation results with the performance metrics of the op-amp



### 4.3.3 Comparator

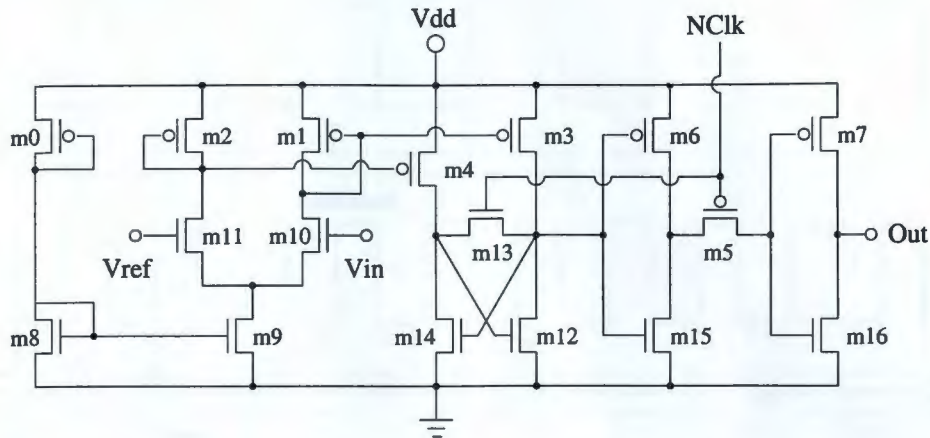


Figure 33. The circuit implementation of Latched Comparator.

The Comparator forms an important component of the SAR ADC, as the performance of the ADC partly depends on the performance of the comparator. A comparator can be thought of as a fast, high gain op-amp which is not used with negative feedback, which compares one analog signal with another analog signal and outputs a binary signal based upon the comparison. A variety of approaches are available to design a comparator but recent studies show that latched comparators are a better choice for modern high speed CMOS applications. Hence the latched architecture was selected for the implementation of the comparator. A latched comparator consists of a preamplifier stage and a latch stage that has two modes of operation: tracking and latching. In the tracking mode, the preamplifier is enabled to amplify the input difference and tracks the input, while the latch is disabled. In the latching mode, the preamplifier is disabled and the latch and the positive feedback are enabled, so that the instantaneous output of the preamplifier is repeatedly amplified and the positive feedback regenerates the analog signal into a full-scale digital signal.

Figure 33 illustrates the comparator circuit implemented in the proposed ADC

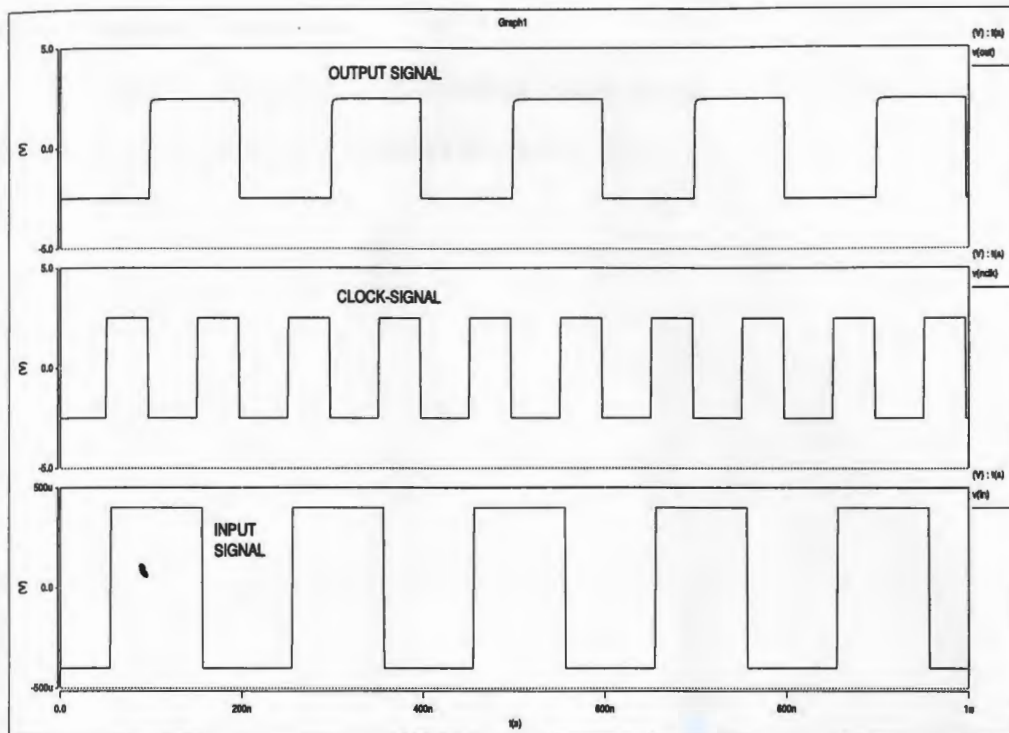


Figure 34. The simulation results of the comparator

design. The output of the accumulator becomes one of the inputs to the comparator and the other input is grounded. Two important performance metrics of the comparator to be considered for the precise operation of the SAR ADC are the comparison rate and the kick back noise. Kick back noise is the power of the transient noise observed at the comparator input due to switching of the amplifier and the latch. As the considered architecture has a preamplifier stage, the effect of the kick-back noise is eliminated. The Figure 34 shows the simulation results of the considered regenerative latched comparator. From SPICE simulations, it is deduced that settling time is about 4ns and it can resolve an input step as small as 0.4 mV. Power dissipation is about 0.4mW. Hence it can be concluded that the considered regenerative latched comparator architecture with strobed output meets the specifications required for precise functioning of the SAR ADC.

#### 4.3.4 Output Registers

The Digital equivalent of the Analog input, which is the output of the comparator are latched using Flip-flop's and latches.

## CHAPTER 5

### Layout and Simulation Results

In this chapter, the initial Floor-planning of the circuit and the various precautions taken while doing the layout to achieve good performance are discussed. Finally the simulation results of the complete SAR ADC are presented.

#### 5.1 Layout Considerations

In the design of mixed signal circuits, several important layout issues should be considered to realize high-quality circuits. Important points to be considered when laying mixed-signal circuits are device matching and noise. Effects of device matching and noise can be reasonably reduced, if proper precautions are taken while laying out the circuit.

##### 5.1.1 Floor Planning

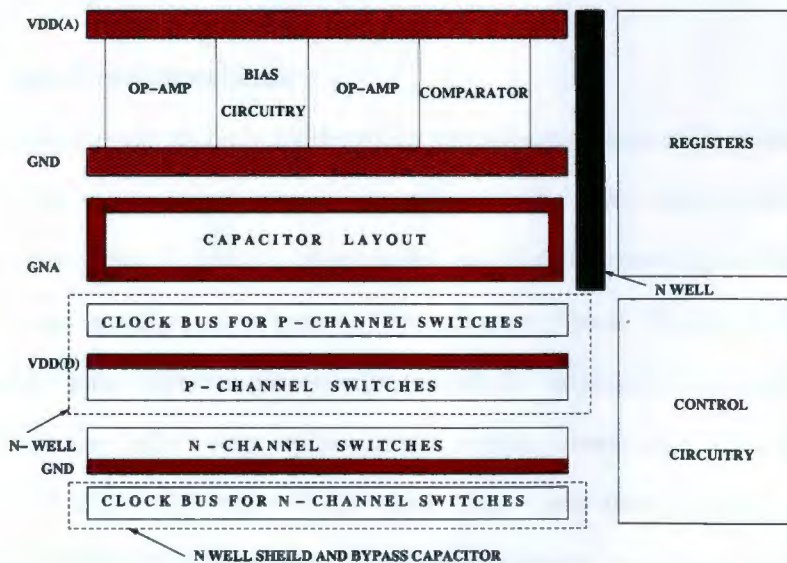


Figure 35. The Floor Planning implemented

A proper planning before laying the circuit isolates most of the sources to

these issues. This process is called Floor-planning. While laying out mixed signal circuits, careful thought should be given to over-all placement of different blocks. Figure 35 illustrates the floor-planning implemented before laying the SAR ADC circuit. As illustrated in the figure, the analog and the digital parts are laid separately to avoid unnecessary injection of noise. The Op-amp and the biasing for the Op-amps are clustered together at the top. Analog capacitors are realized under the op-amp region followed by the MOS switches. The control signals for the switches are laid below the MOS transistors. Thus the control signals or the clocks are placed away from the sensitive op-amps and are also separated using wells and VSS interconnects to avoid injection of clock noise into the analog core. As a good practice, a well is placed under the clock lines as a shield. The shields placed under the analog core and the digital core are also isolated by connecting them to different rails as the shield near the control signals could pick up clock noise. As will be discussed in the next section, different power supply lines are used for both digital and analog parts.

### 5.1.2 Noise Considerations

One crucial issue to be considered in mixed-signal layout is noise. Noise injected into the micro-circuit can be broadly divided into supply-rails noise and substrate noise. Digital circuits inject noise into the surrounding substrate as well as digital power supply rails whenever they change states. To avoid supply noise, it is critical to have different power-supply rails for analog circuits and the digital circuits, which can inject large spikes in the analog power rails. It is a good practice to connect these rails only off the chip. Also, care must be taken to separate the analog interconnects from the digital interconnects as they do not have zero impedance. To minimize the effects of substrate noise, guard rings and wells are placed around the digital and analog parts to create isolation. These help to avoid

the substrate noise from propagating through the resistive substrate. N-wells are used to isolate substrate noise because the doping on the wafer surface is P- type. Additionally, n-well's act as a bypass capacitor and help in lowering the noise on the VDD rails. Finally, after finishing the layout, the unused space must be filled with additional contacts to both the substrate and to the wells which act as the by-pass capacitors as already mentioned.

### 5.1.3 Matching Issues

The effective sizes of the microcircuit components cannot be accurately determined due to a variety of two-dimensional effects introduced during the fabrication. The inaccuracies thus introduced effect the ratio of sizes. This error can be minimized by realizing larger components from a number of unit sized components. Although this approach increased the area, it is usually preferred for the accuracy. As already discussed in the chapter 3 and chapter 4, for the proper functioning of the SAR ADC, precise matching of the capacitors is required. The main sources of errors in realizing capacitors are due to over-etching and oxide thickness gradient across the surface of the microcircuit. The gradient error is minimized by realizing the capacitors by using the common-centroid layout as illustrated in the Figure 36. This realization helps in canceling the gradient effects in both the x and the y directions and thus minimizing the gradient errors. As the number of capacitors required in implementing SAR ADC is less, common centroid implementation is not required as the oxide-thickness variations are reasonably less in a small area.

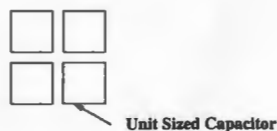


Figure 36. Figure illustrating common centroid layout

## 5.2 Simulation Results

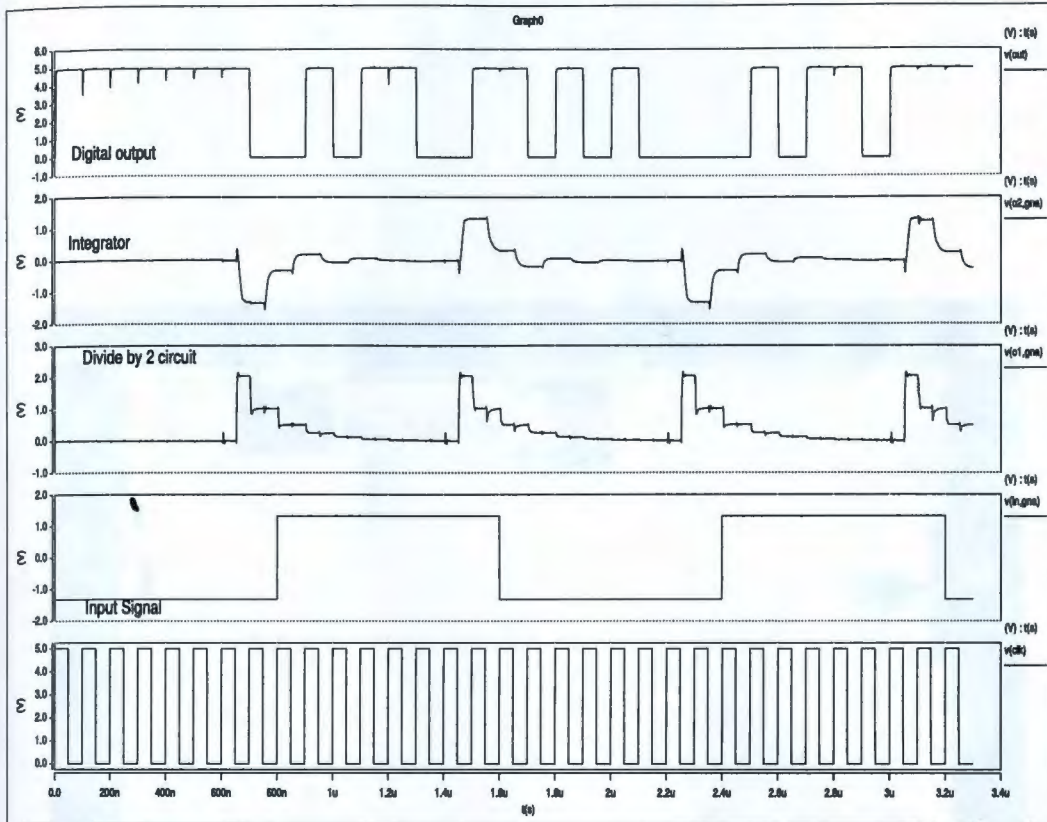


Figure 37. The simulation results of SAR ADC

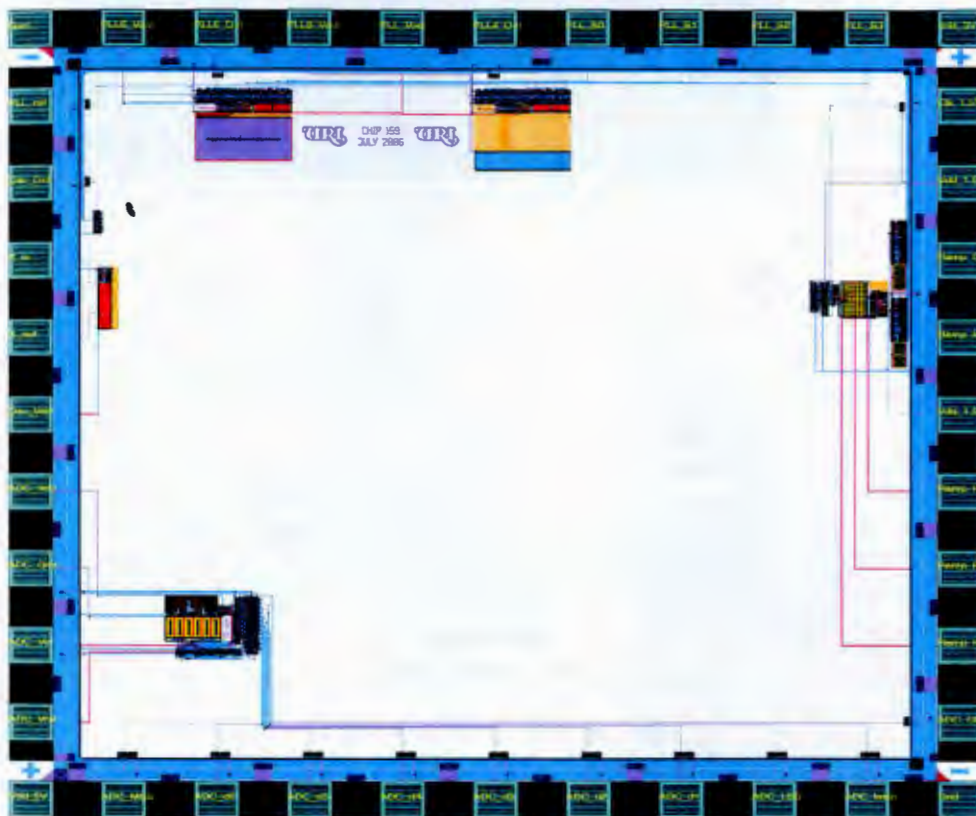


Figure 38. Figure illustrating the complete layout with bonding pads



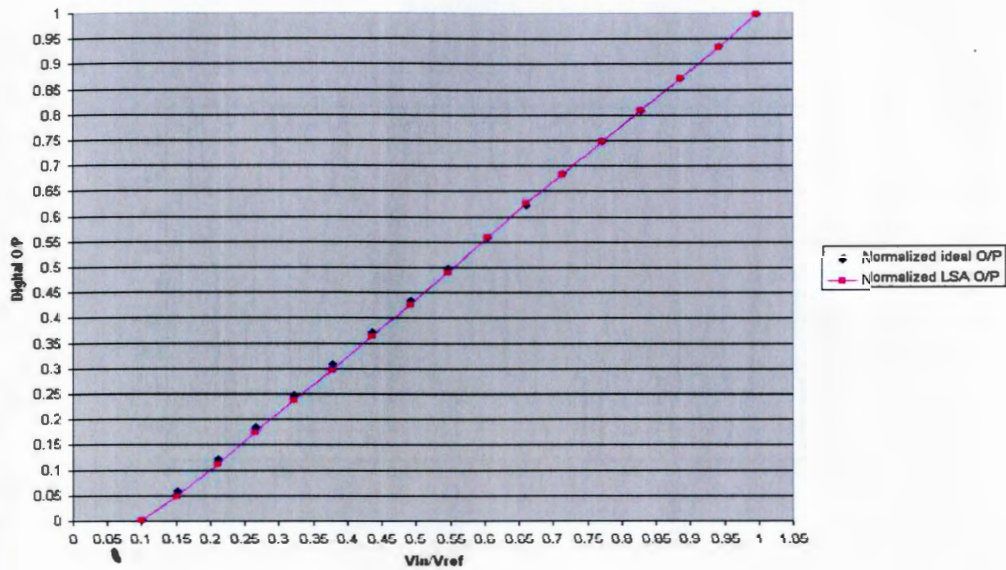


Figure 40. Graph illustrating the Error in LSB's

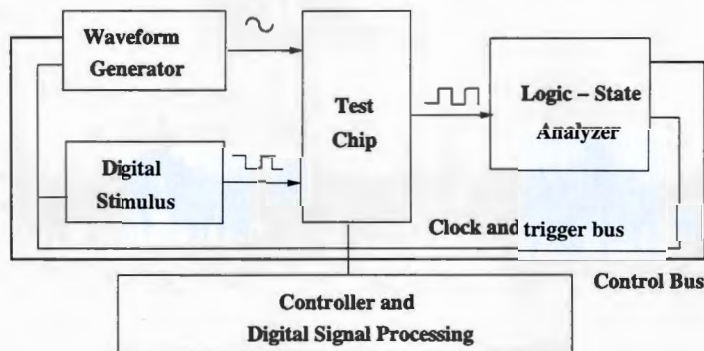
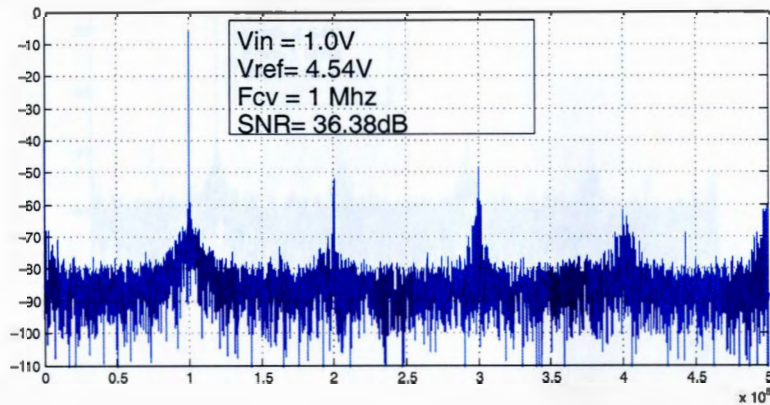
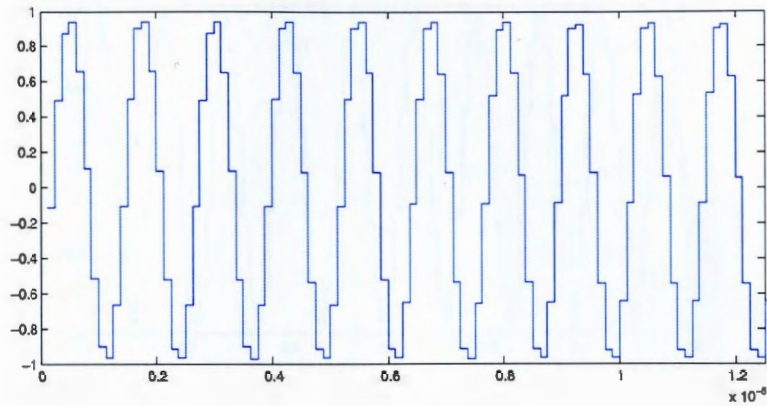


Figure 41. AC Test set-up

Although, DC testing verifies the functionality of ADC, this test does not always reflect the way a converter is used in a real application, where the ADC may have a dynamically changing analog input. The hardware setup for dynamic testing of an ADC requires digital and analog stimuli and digital capture as shown in the Figure 41[1]. A waveform generator is used to provide a sine wave, which serves as the input. The Logic State Analyzer (LSA) stores the output bit stream and thus serves as digital capture. The stream stored in the LSA will be transferred



to a Computer and processed using mathematical tools like MATLAB. One test methodology, to verify the dynamic or spectral characteristics of an ADC is the Fast Fourier Transform (FFT) test[2]. This test can be performed by using signal processing tool-kit in MATLAB, which performs the FFT on the output captured in the LSA. This allows us to calculate the Signal to Noise ratio (SNR) of the ADC, which is evaluates the performance of the ADC. Figure 42 illustrates the FFT results of the data captured from the test chip.

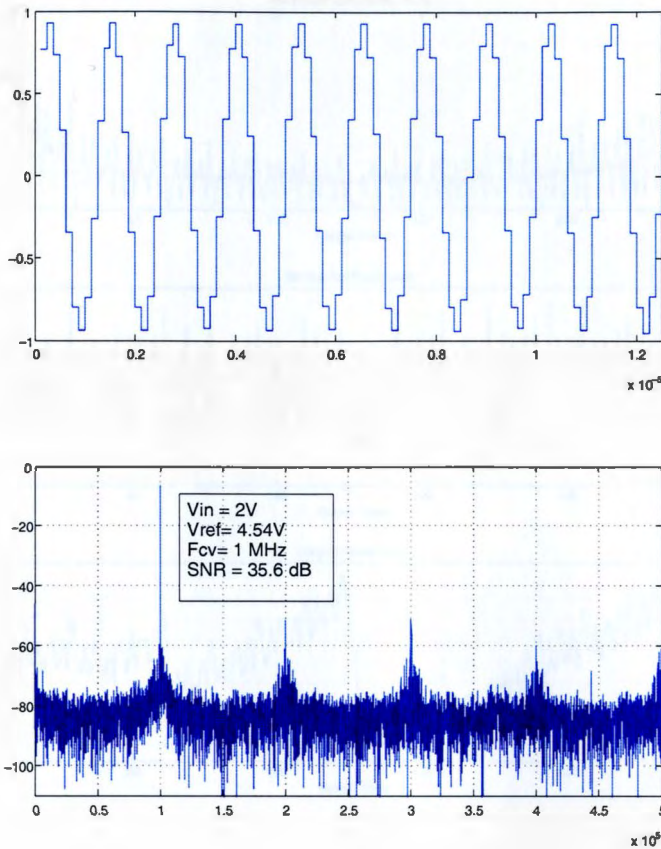


Figure 42. Figures Illustrating the SNR of the test chip

While, FFT Test gives the quantitative analysis of the overall frequency domain measures of the ADC, Histogram Test gives the information on each code transition. Histogram test plots the frequency of occurrence of samples versus possible output codes. Figure 43 illustrates the histogram plot of a set of data captured from the test chip. From the figure, it can be noted that a worse case DNL of about 1.2 LSB is calculated.

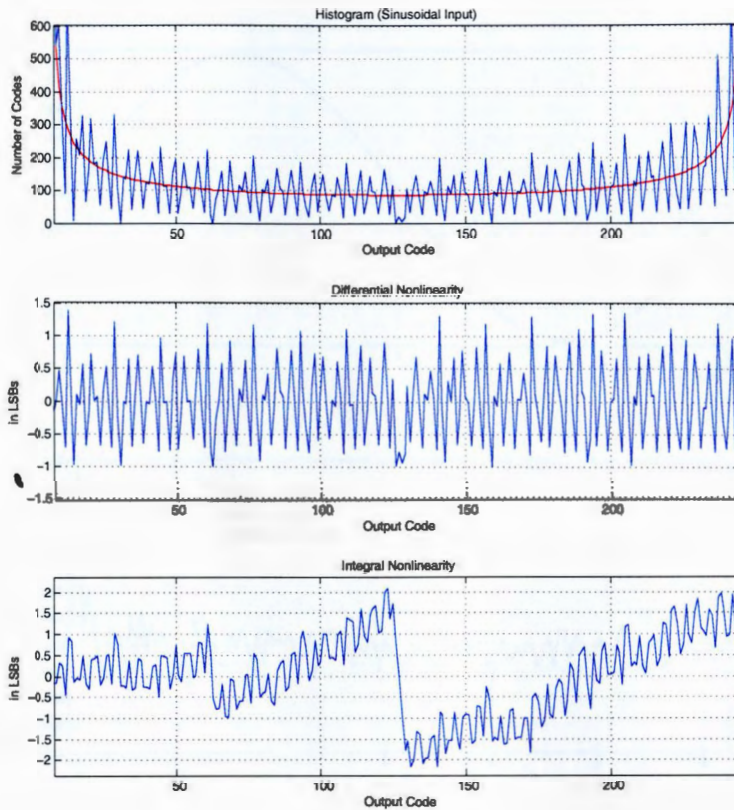


Figure 43. Histogram plot

### 6.3 Conclusion

A Successive approximation ADC with 8-bit resolution and at 1MHz conversion rate was designed and fabricated. The test chip was tested with a clock of 8 MHz and an Effective Number of Bits (ENOB) of 6.2 bits is achieved. From the FFT test, it can be concluded that an average SNR of 38 dB is achieved. The test chip recorded a power dissipation of about 3.2 mW. As a switched capacitor technique is used for the implementation of the ADC, the loss in the resolution is speculated because of the charge injection by the switches in the Divide by 2 circuit

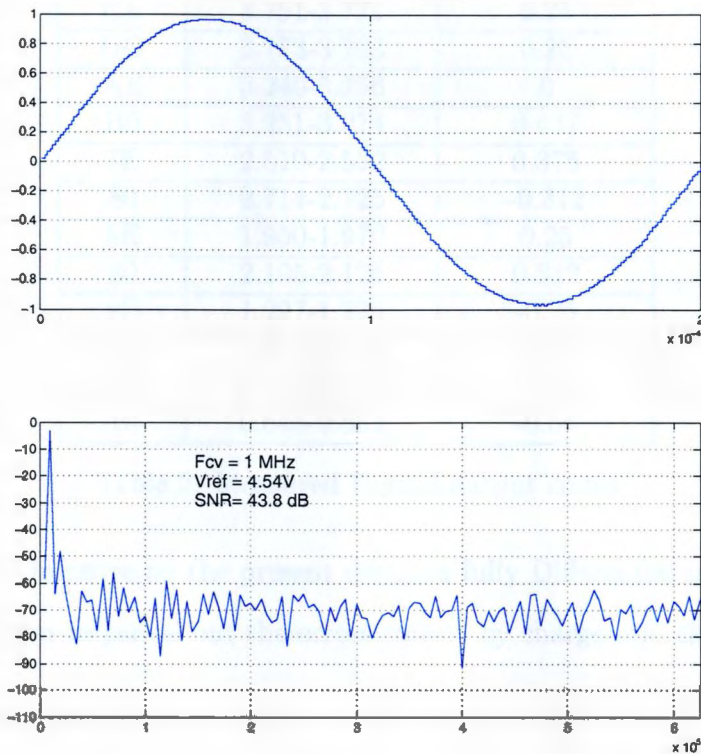


Figure 44. FFT of Spice Extracted File

and in the accumulator. This was also confirmed by the FFT test performed on the extracted spice data. Figure 44 illustrates the FFT test results performed on the extracted spice file. The figure shows that there are missing codes at  $1/2$ ,  $1/4$ ,  $1/8$  etc. trip points. This can be explained by the fact that the channel charge being injected by flipping of each bit is equivalent to 6 mV and thus at the trip points this error exceeds the LSB voltage causing missing codes in the digital output. For example at the  $1/2$  trip point the digital code becomes 10000000 from 01111111, hence the total charge injection in this is around 48 mV thus missing two codes at

Output	Step-size in volts	DNL in LSB's
EE	4.265-4.283	0.125
F0	4.298-4.303	-0.687
CE	3.751-3.771	0.25
DO	3.773-3.793	0.25
AE	3.240-3.256	0
B0	3.251-3.274	0.437
7E	2.510-2.532	0.375
80	2.714-2.725	-0.312
5E	1.950-1.970	0.25
60	2.105-2.126	0.312
2E	1.227-1.239	-0.25
30	1.301-1.311	-0.375
OE	0.716-0.740	0.5
10	0.845-0.852	-0.56

Table 2. Measured Digital output codes

the output. To improve on the present design a fully Differential implementation may be a solution to cancel out the errors caused by charge-injection.

#### List of References

- [1] J. A. Mielke, *Frequency Domain Testing of ADCs*. IEEE Design and Test of Computers, vol. 13, pp. 64-69, 1996.
- [2] C. N. L. Denetazzo, *A/D Converter Performance Analysis By A Frequency Domain Approach*. IEEE Transactions on Instrumentation and Measurement, vol. 41, pp. 285-288, 1992.

## BIBLIOGRAPHY

- Chi-Sheng Lin, B.-D. L., "A new successive approximation architecture for low-power low-cost cmos a/d converter." in *IEEE Transactions on Circuits and Systems*, 2003, pp. 54-62.
- Cliffs, E., *Devices, Analog-Digital Conversion Handbook*. New Jersey, United States of America: Prentice Hall, 1996.
- Daugherty, K. M., *Analog-To-Digital Conversion: A Practical Approach*. New York, United States of America: McGraw-Hill Inc, 1994.
- David A. Johns, K. M., *Analog Integrated Circuit Design*. New York, United States of America: John Wiley and Sons, 1997.
- Jackson, L. B., *Digital Filters and Signal Processing*. Boston, United States of America: Kluwer Academic Publishers, 1995.
- John.g Proakis, M. S., *Fundamentals of Communication Systems*. Upper Saddle River, New Jersey, United States of America: Prentice Hall, 1998.
- Kennedy, M. P., "On the robustness of r-2r ladder dac's." in *IEEE Transactions on Circuits and Systems*, 2000, pp. 109-116.
- Kenzo Watanabe, G. C. T., "A switched capacitor multiplier/divider with digital and analog outputs." in *IEEE Transactions on Circuits and Systems*, 1984, pp. 796-800.
- Lenk, J. D., *Simplified Design of Data Converters*. Boston, United States of America: EDN series for Design Engineers, 1996.
- Mielke, J. A., "Frequency domain testing of adcs." in *IEEE Design and Test of computers*, 1996, pp. 64-69.
- Razavi, B., *Data Conversion System Design*. New York, United States of America: IEEE Press, 1995.
- R.J Baker, Harry W. Li, D. B., *CMOS circuit Design, Layout and Simulation*. New York, United States of America: IEEE Press Series on Microelectronic Systems, 1998.
- Siamak Mortezapur, Edward K, F. L., "A 1-, 8-bit successive approximation adc in standard cmos process." in *IEEE Journal of Solid-State Circuits*, 2000, pp. 642-646.

Siamak Morteza pour, E. K., *A 1-V, 8-Bit Successive Approximation ADC in standard CMOS Process.* IEEE Journal of Solid-State Circuits, vol. 35, No. 4, pp. 642-646, 2000.